

# Human Response to Acceleration

Robert D. Banks, James W. Brinkley, Richard Allnutt, and Richard M. Harding

The most reliable instrument for measuring the varied effects of dynamic force on man is man.

—Colonel John Paul Stapp

The first principle is that you must not fool yourself and you're the easiest person to fool.

—Richard Feynman

## INTRODUCTION

Acceleration is the rate of change of velocity. The human response to acceleration depends on magnitude, direction, and duration. The response may be physiological and involve homeostasis during accelerations of low magnitude and long duration. Or it may involve physical injury when the acceleration is high and of short duration. These two general outcomes characterize the way human response to acceleration has been considered, studied, and analyzed.

Low-magnitude, long-duration acceleration involving humans has been termed *sustained acceleration*. High-magnitude, short-duration acceleration has been termed *impact* or *transient acceleration*. In this chapter, we consider the effects of both sustained and impact acceleration on humans and some of the protective strategies associated with each. Because sustained acceleration is encountered by pilots in flight and the major threat is incapacitation, the aim of protection is to prevent a crash and enhance flying ability. Because transient acceleration is encountered during flight operations, escape, or during a crash, the aim of protection is to maintain function, reduce injury potential, and enhance survivability.

These two areas employ very different research methods: one involves mainly human centrifuges and the other, impact tracks and towers. Both approaches have limitations in their ability to simulate real-world events. Models, based

on appropriate research, have been developed according to the principles of Newtonian mechanics. We begin with a review of these principles.

### Newton's Laws

Newton's first law states that a body that is at rest or in motion will remain in that state unless acted upon by a force. A force is a push or pull. For example, an aircraft in straight and level flight is without acceleration if the forces acting on the aircraft are in balance. Similarly, occupants of the aircraft are without acceleration, although they will experience the force of gravity by virtue of lift of the wings.

If an aircraft follows a curving path, such as during a banked turn or upward pitch, a force must act on the aircraft to alter its path (in this case, forces due to lift). In Figure 4-1, the aircraft pitches up due to the forces of lift.

Occupants inside the aircraft also follow Newton's first law and therefore follow a straight path at a constant velocity unless acted upon by a force. During a banked turn or upward pitch, this force is exerted on the occupant by the seat and floor of the aircraft as illustrated in Figure 4-1.

In Figure 4-2, we illustrate the case of an aircraft pitching down. In this example, the occupant is experiencing a fall to Earth and is also being pulled down by the lap and shoulder belts.

When an aircraft impacts the ground during a crash, the velocity of the aircraft changes abruptly and the aircraft

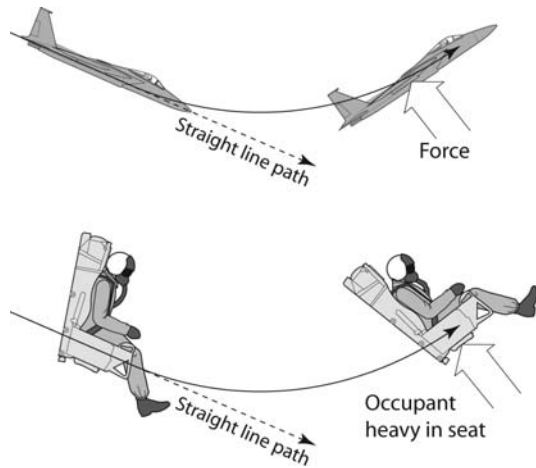


**FIGURE 4-1** Newton's first law. The aircraft will continue in a straight path unless acted upon by an unbalanced force. When the aircraft follows a curving path, the unbalanced force is due to lift. The occupant will also follow a straight path unless acted upon by an unbalanced force. In this case, the force is the aircraft acting upwards on the pilot (Source: John Martini, BRC).

experiences deceleration. In accordance with Newton's first law, the occupants of the aircraft will continue at their preimpact velocities until they contact interior aircraft structures that are slowing. In a frontal impact, the first such structure is the restraint system. The next structure will be the instrument panel or control column. Figure 4-3 shows a pilot immediately before the aircraft contacts water. As depicted, during the impact event, the pilot experiences motion within the cockpit interior and contacts forward structures.

Newton's second law relates force and acceleration, and is expressed as:

$$F = ma \quad [1]$$

where  $F$  = force,  $m$  = mass,  $a$  = acceleration.

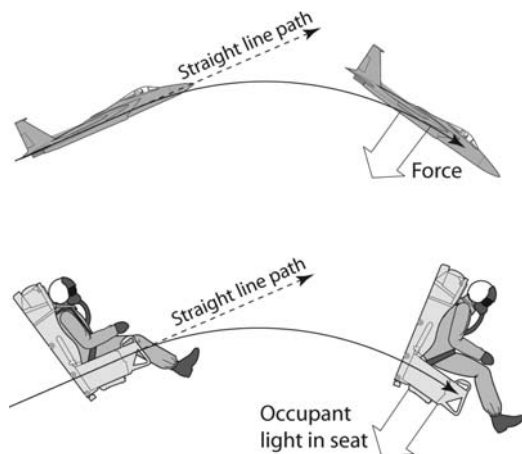


**FIGURE 4-2** Newton's first law applied to an occupant in flight. The force acting on the occupant is downward through the lap and shoulder restraints. The occupant will tend to rise out of the seat (Source: John Martini, BRC).

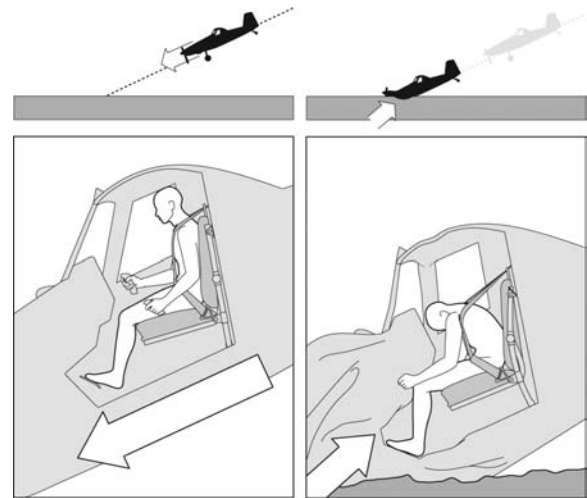


**FIGURE 4-3** Newton's first law applied to an occupant during a crash. The occupant will continue at the precrash velocity during the event until encountering objects forward of the initial position. In this case, these objects include the restraints, controls, and the instrument panel. As seen from within the aircraft, occupant motion appears to be forward (Source: John Martini, BRC).

We can see from Newton's second law that when acceleration increases so does force, and *vice versa*. When a force is applied to an occupant through the seat or restraint, the occupant experiences both acceleration and force. In the case of frontal impact with terrain, the occupant experiences acceleration and force due to contact with the restraints and forward cockpit structures.

Newton's third law states that any force exerted by one body on another is countered by an equal and oppositely directed force. Because colliding objects usually have different masses, the resulting accelerations will not be the same (Newton's second law).

## Understanding G

The acceleration due to gravity is the same (constant) anywhere on the surface of a planet although it decreases with increasing distance from the center. On Earth, this constant is designated "g" and has the value of approximately 9.81 meters/second squared ( $m/s^2$ ). The force that an object exerts on the Earth's surface (weight) depends on the mass of the object, but will be the same anywhere on the Earth's surface for that mass.

The situation is different on other planets. On our moon, for example, acceleration due to gravity is only  $1.62 m/s^2$  and an object will fall to the lunar surface with less acceleration than on Earth. Similarly, the weight of an object on the moon's surface is less than that of the same object on Earth. A person who weighs 78 kilograms (kg) on Earth will weigh only 13 kg on the moon.

Gravity also affects objects in space that are close to the Earth. Gravity causes spacecraft and their occupants to fall toward the Earth. Spacecraft that have achieved orbital velocity during launch (8 km/s) circle the Earth. Because the Earth's surface curves away from their path (being round),

the spacecraft and crewmembers cannot close the distance to the surface and so remain in semiperpetual freefall. The “weightlessness” of Earth’s orbit is not the absence of gravity; it is a condition of frictionless freefall.

“G” is a measure of the acceleration experienced by a person as a result of a force. Alternatively, it can be regarded as a measure of the force experienced by a person due to acceleration. It is expressed in terms of multiples of the Earth’s gravitational acceleration. One G is experienced during acceleration of  $9.81 \text{ m/s}^2$  (g).

The relationship of G and acceleration can therefore be expressed as:

$$G = a/g \quad [2]$$

Because both “a” and “g” have units of  $\text{m/s}^2$ , and they are divided, the units cancel and G is without units—it is a ratio.

As stated, the G coefficient relates to force. For example, a pilot weighing 70 kg on Earth who is subject to an in-flight acceleration of 3 G (and is supported by the seat and restraints), will experience a force that is three times his weight, or 210 kg. It is often more practical to discuss G instead of force or acceleration because force measurements vary with pilot mass, but acceleration does not. *Acceleration* is convenient to consider in terms of multiples of gravity, and is the term used by aircrew and flight surgeons in the aviation community.

## Vectors and Nomenclature

Any quantity that has the properties of magnitude and direction is called a *vector*. Acceleration, velocity, and force are examples of vectors. G is also a vector. Vectors can be analyzed mathematically using trigonometry. Vectors are described on plots that demonstrate their magnitude and direction. These plots are defined by three mutually orthogonal linear axes: x, y, and z. In aerospace medicine, these plots are considered to be aligned with a forward-facing crewmember as depicted in Figure 4-4.

There has been considerable disagreement about both the conventional placement of axes, and the use of symbols and terms. Basic differences exist between the engineering and aeromedical communities, and within each of these groups. Attempts to achieve uniformity have had mixed results. For example, the Advisory Group for Aerospace Research and Development (AGARD) standard for human acceleration differs from the AGARD standard for aircraft design (in which the z-acceleration axis is reversed and positive downward). It also differs from previous editions of this textbook, which differ from one another. Needless to say, when reading literature involving acceleration it is important to understand clearly the author’s use of these terms and symbols.

To be consistent with the AGARD standard (1), the Table of Equivalents for Acceleration Terminology (2), the Aviation Space and Environmental Medicine Standard (3), and the majority of the Aerospace Medicine literature, the positive direction of each of these axes is here described by “the left-hand rule.” That is, the x-axis dimension is an arrow

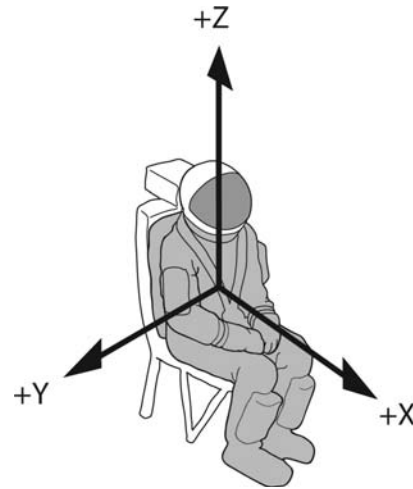


**FIGURE 4-4** An axial diagram of the human coordinate system for linear motion. This convention is referred to as the *left-hand rule* because the placement of the axes mimic a left hand with the index finger pointed forward, the thumb pointed up, and the middle finger directed to the right (Source: John Martini, BRC).

with the positive direction forward, the y-axis dimension has the positive direction rightward, and the z-axis dimension has the positive dimension upward. This is depicted in Figure 4-4.

Aircraft acceleration vectors can be described using this convention. If an aircraft accelerates forward, in the positive direction, the acceleration is denoted by “ $+a_x$ ”. If the direction of aircraft acceleration is upward, the designation  $+a_z$  is used. If the direction is to the right,  $+a_y$  is used. These symbols are included in the first column of Table 4-1.

The positive direction of the G of an occupant in response to aircraft acceleration is aligned with a. Therefore, when  $+a_x$  is experienced by the aircraft, a forward-facing occupant experiences  $+G_x$ . Otherwise stated,  $+G_x$  is caused by acceleration of the seat forward and results in pressure between the seatback and the pilot’s back.  $+G_y$  is caused by acceleration of the seat toward the right and results in pressure between the left hip and the left armrest. Positive  $-G_z$  is caused by acceleration of the seat upward and results in pressure between the buttocks and the seat pan. These conventions and their counterparts are summarized in Table 4-1. In column 3,

**TABLE 4 - 1**

**Directions of Acceleration and Use of Terms**

Acceleration	Cause G	Description
$+a_x$	$+G_x$	“Step on the gas”
$-a_x$	$-G_x$	“Step on the brakes”
$+a_y$	$+G_y$	Pressure against left arm rest
$-a_y$	$-G_y$	Pressure against right arm rest
$+a_z$	$+G_z$	Heavy in the seat
$-a_z$	$-G_z$	Light in the seat

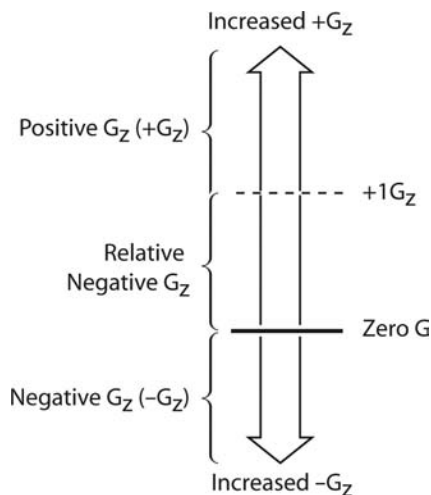


**FIGURE 4-5** Vertical accelerations greater than  $+1 G_z$  are termed *positive- $G_z$*  ( $+G_z$ ). Any  $+G_z$  less than  $+1 G_z$  is termed *relative- $G_z$* . Any  $G_z$  less than zero- $G_z$  is termed *negative- $G_z$*  ( $-G_z$ ) (Source: John Martini, BRC).

we have included phrases that may aid in understanding these conventions. The symbol “G”, without a subscript letter or prefix symbol, is used when the direction is not specified.

Another source of confusion is associated with the  $+1 G$  of gravity. An aircraft at rest on the Earth, or in straight and level flight, experiences  $+1 G_z$ , and yet there is no acceleration. Therefore, the zero-acceleration reference point in the z-direction is  $+1 G_z$  because of gravity. Because any  $G_z$  less than  $+1 G_z$  is *relatively negative*, in terms of the effect on an upright human, we use the term *relative- $G_z$*  to describe  $G_z$  stress that is less than  $+1 G_z$ , but greater than zero- $G_z$ . When  $G_z$  is less than zero- $G_z$ , the expression “negative- $G$ ” or “ $-G_z$ ” is used. Confusion can occur when thinking of less than  $+1 G_z$  and greater than zero- $G_z$ . Although this is technically  $+G_z$ , physiologically, the body responds as if it is  $-G_z$  because the autonomic nervous system is adapted to gravity. Figure 4-5 illustrates this definition.

### Frames of Reference

To have proper meaning, the orthogonal linear axes used to describe vectors must be defined according to a “frame of reference.” For example, a person sitting on a train traveling at a constant velocity of 100 Kmph would perceive no speed inside the train and that would be indicated on a vector plot referenced to the inside of the train. An observer positioned in an alternate frame of reference, such as outside the train at a station, would see the person in the train speeding past at 100 kmph, and a vector plot referenced to the station would reflect this velocity. Although describing the same event, the vectors would look quite different because of the different frames of reference.

Any vector, including force, velocity, and acceleration (or G) depends on the frame of reference selected. Sustained acceleration is usually considered within the reference frame of the aircraft interior and occupant space. Transient

acceleration is often considered within the reference frame of the Earth.

G is measured using an instrument called an *accelerometer*, or *G-meter*. Many aircraft have G-meters mounted on the aircraft and positioned in the cockpit, where they can be seen by the pilots. The G-meter is calibrated to measure acceleration in the aircraft reference frame ( $a_z$  in units of  $G_z$ ). Similarly, human centrifuges, used to create G on Earth, often have accelerometers mounted near the occupant seat.

## PHYSIOLOGY OF SUSTAINED ACCELERATION

Sustained acceleration occurs during normal and aerobatic flight. Because most aircraft maneuvers (such as pitch and banked turns) expose seated occupants to predominantly  $+G_z$ , the effects of  $+G_z$  on humans has received most of research attention. Negative- $G_z$  has received much less attention, most of it during and shortly after World War II.  $G_x$  and zero-G are most relevant to space flight.  $G_y$  has only begun to receive research attention with the development of vectored thrust fighters.

This section describes the effects of sustained G in present-day aviation and space flight. Countermeasures are described and limitations in current research are discussed. The need for a revised model of  $+G_z$  tolerance is suggested.

### Relevant Mechanics

Humans respond physiologically to G. When an aircraft follows a curving path, the velocity changes continuously along the curve (being a vector, although speed may remain constant) and the aircraft experiences acceleration. The acceleration of the aircraft depends on the velocity of the aircraft and the radius of the turn. This is expressed as:

$$a = v^2/r \quad [3]$$

where  $v$  = velocity,  $r$  = radius of the turn.

If the aircraft occupants are “fixed” to the aircraft, they experience the same acceleration, which is expressed as:

$$G = v^2/rg \quad [4]$$

When an occupant experiences  $+G_z$ , the associated force is felt as increasing pressure of the buttocks against the surface of the seat. The occupant experiences “heaviness,” and activities, such as lifting an arm, will be more difficult. When relative  $-G_z$  is experienced, there is a reduction in pressure on the buttocks and the occupant may feel a rise off the seat. As  $-G_z$  increases, pressure of the shoulder and lap restraints is experienced. Ultimately, the occupant may feel suspended by the shoulders and have the sensation of being inverted.

Some aircraft, including civilian aerobatic and military aircraft, are capable of executing large pitch changes at relatively high velocities and can therefore generate high  $G_z$ . The magnitude and duration of  $G_z$  that an aircraft generates depends on its structural strength and thrust.

Incidentally, Equation 3 can be used to calculate orbital velocity. In stable circular orbit, the acceleration of gravity is equal and opposite to the acceleration due to radius of turn. With a low-Earth orbital radius of 6,700 km, it is easy to show that the turn velocity necessary to create 1 G in opposition to the 1 G of gravity is approximately 8 km/s, which is the low-Earth orbital velocity previously mentioned. This orbital balance of acceleration vectors is a special and important case of weightlessness. Both the freefall concept and the acceleration balance concept are useful and correct in understanding orbital weightlessness.

## The Fluid Model

When force is applied to fluid in a constrained volume, the pressure within increases. Pressure is a measure of force (per unit area) transmitted by fluids. For example, squeezing a filled plastic water bottle increases the pressure of the water inside the bottle. If the top is off, the increased water pressure compels the water to squirt out against the constraint of gravity and the resistance of the opening. Similarly, heart contraction during systole increases the pressure within the left ventricle and compels high-pressure blood to open the aortic valve and flow into the aorta.

On Earth, the force acting on a fluid at any depth varies with the weight of the fluid above, a principle of hydrostatics. Therefore, pressure increases with increased depth, a fact well known to divers. Referring to the depiction of the column of fluid in Figure 4-6, we expect the pressure of fluid to be less at point A than at point B because there is no fluid *above* point A. Because fluids are freely mobile, and have no internal rigid structure, pressure is transmitted within the fluid according to Pascal's principle (which states that a change in pressure at any point in a fluid is transmitted to every part of the fluid).

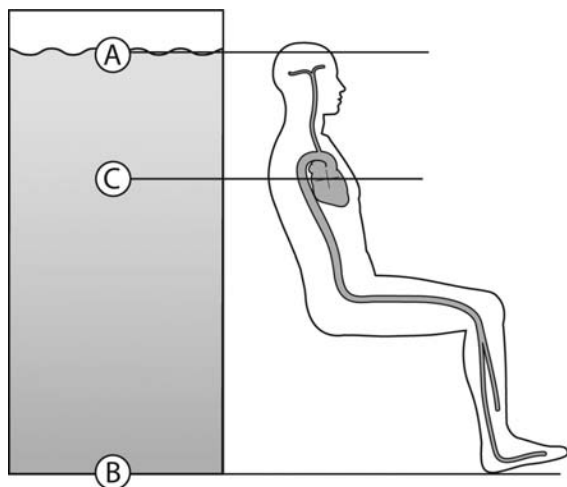


**FIGURE 4-6** Hydrostatic blood pressure. A seated human figure is depicted next to a fluid-filled container. The hydrostatic pressure of the fluid is zero at the top of the container (A), and maximum at the bottom (B). The pressure is intermediate at point C, which is located between A and B. These principles apply equally to the fluids of the human figure seated to the right (Source: John Martini, BRC).

Hydrostatic principles apply to all fluids in the body, including the pericardial, pleural, abdominal, and cerebrospinal fluids, and both venous and arterial vascular systems. To the right of the water column in Figure 4-6, we present a seated upright human, and depict the continuous fluid column (cardiovascular system) that extends from the scalp to the feet. Ignoring any pressure generated by the heart, and considering only the hydrostatic pressure of the fluid column, blood pressure at level A is zero, because there is almost no blood above. Blood pressure at the feet (level B) is greatest and equal to the weight of the fluid above. At level C, blood pressure measured at the heart, is intermediate. This component of blood pressure is termed the *hydrostatic* pressure component.

Pressure due to contraction of the heart adds to the hydrostatic component of blood pressure. If we consider left ventricular contraction during systole, the force applied to the contained blood by cardiac muscle increases intraventricular blood pressure until the aortic valve opens. The increased blood pressure is then transmitted to the aorta and into the arterial system according to Pascal's principle. This component of blood pressure is termed the *dynamic* pressure component.

Total blood pressure is the sum of the dynamic and hydrostatic pressures. The measured systolic blood pressure at the heart level of a young healthy adult is typically approximately 120 mm Hg and is the sum of the two blood pressure components. Measurements taken at other vertical locations (e.g., the ankle) will be different.

Numerical estimates of hydrostatic blood pressure can be made using Equation 5, which states:

$$p = \rho gz \quad [5]$$

where  $p$  = hydrostatic pressure,  $\rho$  = blood fluid density,  $z$  = vertical depth of fluid.

For a specific gravity of blood of 1.06, and after converting the units of  $p$  from Pascals to millimeters of mercury (mm Hg), Equation 5 becomes:

$$p = 0.78z \quad [6]$$

where  $p$  is in mm Hg, and  $z$  is in cm.

Equation 6 can be used to estimate the hydrostatic component of blood pressure at different vertical fluid column depths on Earth (+1  $G_z$ ). For example, if the vertical distance from the aortic valve to the top of the head is 38 cm, Equation 6 predicts that the hydrostatic pressure at the aortic valve in an upright person is approximately 30 mm Hg ( $0.78 \times 38$ ).

As  $G$  increases, the apparent weight (force) of any object increases directly, and this applies equally to fluids. Under increased  $G$ , Equation 6 becomes:

$$p = 0.78zG \quad [7]$$

Equation 7 can be used to predict  $G$ -tolerance, if physiological compensation is not considered. For example, an individual with a vertical fluid distance of 38 cm from the aortic valve to near the top of the head, and having a systolic blood pressure

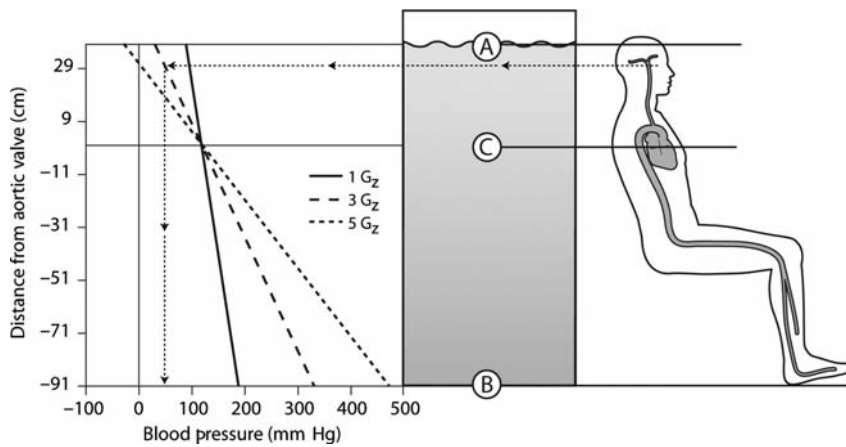


**FIGURE 4-7** The estimated blood pressures are plotted next to a depiction of a seated human figure using Equations 6 and 7 (assuming a heart-level systolic blood pressure of 120 mm Hg and a 50% average male). To determine the blood pressure at any vertical location, a horizontal line can be run toward the left to the straight line plot of  $+G_z$ . The pressure is read directly below on the horizontal axis. The arrowed line provides an example of how to estimate the blood pressure at eye-level during exposure to  $+3 G_z$ . Note the high blood pressures in the lower extremities and predictions of head-level blood pressures at  $+5 G_z$  that are less than atmospheric (Source: John Martini, BRC).

at the aortic valve of 120 mm Hg, would be expected to have zero systolic blood flow near the vertex at approximately  $+4 G_z$  [Equation 7:  $120 \text{ mm Hg} = 0.78(38)(4.0)$ ]. This is a point above which the dynamic systolic blood pressure is unable to oppose the hydrostatic component of the blood. Consequently blood flow to the upper brain would cease.

Equation 7 can also be used to estimate blood pressures at other locations. Figure 4-7 shows the person seated upright as depicted previously in Figure 4-6. To the left of the human figure are plots of systolic blood pressures versus distance from the aortic valve based on Equations 6 and 7. There are three plots depicted:  $+1 G_z$ ,  $+3 G_z$ , and  $+5 G_z$ , and they are based on the approximate dimensions

of a 50% average male. Any estimates, using this simple model, will vary with individuals of different sizes. Note the very high blood pressures in the lower extremities at  $+5 G_z$ . Similarly, pressures at head level are predicted to be less than atmospheric pressure at  $+5 G_z$ . Once again, the underlying assumption is a heart-level systolic blood pressure of 120 mm Hg.

Equation 7 can be used for other postural orientations such as reclined or inverted. Figure 4-8A depicts the expected blood pressures for a seated reclined individual. Because of the reclined posture, the vertical heart-to-brain distance is decreased, and the hydrostatic blood pressure component is less. Positive- $G_z$  tolerance is predictably

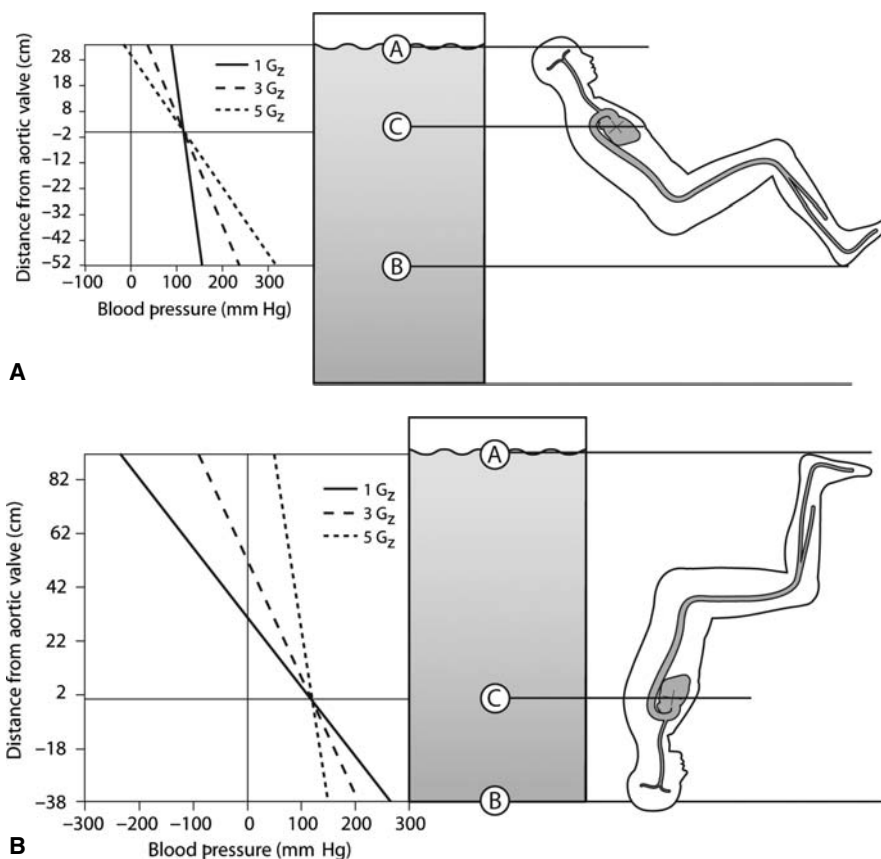


**FIGURE 4-8 A:** The estimated systolic blood pressures when the seated individual is reclined during  $+1 G_z$ ,  $+3 G_z$  and  $+5 G_z$  exposure. By reclining the seatback, the vertical dimension of the hydrostatic column is reduced and hydrostatic pressure above the heart is reduced. Positive- $G_z$  tolerance is predictably improved (Source: John Martini, BRC).

**B:** The estimated systolic blood pressures when the seated individual is exposed to  $-1 G_z$ ,  $-3 G_z$  and  $-5 G_z$  (inverted). This posture depicts increased levels of  $-G_z$ . Note the very high predicted head-level systolic blood pressures (Source: John Martini, BRC).

increased. Figure 4-8B demonstrates the effect of inversion, and also the very high head-level blood pressures that can be experienced during  $-G_z$ .

These predictions agree well with human studies that show a head-level reduction of blood pressure of approximately 30 mm Hg per change of each 1 G (4).

Blood pressure at the head is further lowered if circulating blood volume is reduced. When blood pressure increases during increased  $+G_z$ , as it does in the lower (dependent) areas of the body (Figure 4-7), stretching of tissues occurs. As a result of stretching of tissues in the abdomen and lower extremities, a portion of the circulating blood volume becomes unavailable for circulation.

Individual variations in heart-to-brain distances, and differences in blood pressures at the aortic valve, will change these predictions. Therefore, people with smaller vertical dimensions when upright will have an advantage tolerating  $+G_z$  when compared to taller people. Elevation of blood pressure at the aortic valve would predictably increase  $+G_z$  tolerance.

## Human Physiological Response to G

### Positive Vertical Acceleration ( $+G_z$ )

The brain is very sensitive to cellular hypoxia, which produces rapid loss of brain function. Because oxygen is transported to the brain through the cardiovascular/respiratory system, any interruption in arterial blood flow to the brain leads to cerebral hypoxia. However, loss of function does not occur immediately, when blood flow ceases. There is a reserve time of approximately 4 to 6 seconds before loss of brain function begins (5,6).

Physiological control of blood pressure is based (in part) on the closed-loop baroreceptor reflex. Consisting of upper thoracic and carotid body receptors, efferent and afferent nerves, and centrally mediated responses, the baroreceptor reflex controls blood pressure through activation of the autonomic nervous system. When *decreased* transmural pressure is sensed in the upper thorax and carotid bodies, the sympathetic nervous system (pressor response) is activated. When *increased* blood pressure is sensed in the upper body, the parasympathetic nervous system (depressor response) is activated.

The sympathetic nervous system raises blood pressure by increasing its dynamic component. The dynamic component of blood pressure is related to heart rate, stroke volume, and total peripheral resistance. Elevated heart rate and stroke volume both cause blood pressure to increase by raising the volume and pressure of blood injected into the arterial system. Total peripheral resistance is increased when arterial smooth muscle constricts and thereby reduces the circulating arterial blood volume space.

Although very effective in compensating for upper body hypotension, the baroreceptor reflex takes time, on the order of 6 to 9 seconds, with heart-level blood pressure restored in 10 to 15 seconds (7). This compensatory response is therefore slower than the cerebral hypoxia reserve time of 4 to 6 seconds. If sufficient  $+G_z$  is experienced, the

sympathetic response is inadequate and cerebral hypoxia occurs. A measure of autonomic nervous system response to  $+G_z$  is heart rate, which increases directly with increased  $+G_z$  level, reaching a maximum within a few seconds of exposure. High-sustained  $+G_z$  exposures usually result in a maximum heart rate of approximately 170 beats/minute.

In contrast, the parasympathetic nervous system attempts to lower upper body blood pressure by decreasing heart rate, stroke volume, and total peripheral resistance. This general relaxing of myocardial and vascular tissues occurs quickly, in comparison to the sympathetic nervous system response, and can be fully developed within 2 to 4 seconds (8,9). During  $-G_z$ , heart rates fall dramatically: reductions of 50 beats/minute have been recorded during exposures of  $-3 G_z$  with some subjects experiencing brief periods of asystole (10).

Adequate cardiac output depends on the supply of blood to the heart through venous return. Although the fluid model might predict that venous return is diminished during increased  $+G_z$ , early experiments determined that the abdominal contents (as a whole) behave like an enclosed fluid, and that venous return is generally maintained (7).

In addition to the baroreceptor response, sympathetic nervous system dominance is facilitated by the endocrine system. Physiological responses to air combat, aerobatics, centrifuge experiments, or any unusual G-exposure elicit an immediate “fight or flight” response with increased levels of epinephrine, norepinephrine, and serum cortisol (11). The endocrine response is slower than the baroreceptor reflex, but becomes important as G exposures increase in duration.

The respiratory system is also affected by increased  $+G_z$ . As hydrostatic pressures increase during increased  $+G_z$ , lung perfusion is redistributed toward the base of the lung, especially at relatively low G levels. During acceleration, the alveolae, owing to the vast differential in specific density between blood and air, expand at the top of the lung while those at the base of the lung, where most blood has moved, become smaller with some collapsing (12). As a result, ventilation/perfusion mismatch and acceleration atelectasis can occur. These responses are further described in Chapter 2.

Increased abdominal pressure during  $+G_z$  also prevents full descent of the diaphragm. This impairs vital capacity because of a reduced inspiratory capacity (12). Lung compliance decreases and results in an increased resistance to changes in volume. Reduced compliance and increased weight of the chest wall structures increase the work of respiration in proportion to increased  $+G_z$ . A total increase of 55% in the work of breathing occurs at  $+3 G_z$ . Further details are provided in Chapter 2.

At one time, aerospace physiologists were concerned that human exposures to greater than  $+9 G_z$  could lead to lung tissue injury. These fears have been proved unfounded, at least up to  $+12 G_z$  (13). Former concerns about poor blood oxygenation also proved unfounded, possibly because the major physiologic demands during exposure to G are anaerobic, with physiologic limitations caused by fatigue.

## Symptoms and Signs of Uncompensated +G<sub>z</sub> Stress

### Visual

As +G<sub>z</sub> increases, the first symptoms experienced usually consist of visual changes. The interior of the eye is enclosed and normally has an internal pressure of 10 to 21 mm Hg. The retinal artery pierces the posterior globe and enters the central retina with the optic nerve. For retinal blood perfusion to occur, arterial pressure must be greater than the internal eye pressure. If it is not, retinal ischemia occurs, first at vessels farthest from the optic disc and then with progression toward the central retina.

A pilot in flight who is exposed to increasing +G<sub>z</sub> can experience dimming of vision, starting at the visual periphery. This is termed *tunnel vision* and is familiar to most pilots who have been trained to expect it. In the presence of continued (and increased) +G<sub>z</sub>, visual symptoms can progress inward from the periphery to include the central vision, a symptom known as *gray-out*. Not all air crew experience loss of peripheral vision before central vision. If +G<sub>z</sub> is reduced, restoration of vision occurs quickly.

With continued or increased +G<sub>z</sub>, visual symptoms can progress from gray-out to complete loss of vision, or “blackout” (not to be confused with loss of consciousness). Brain and auditory functions remain undisturbed if there is no further decrease in brain-level blood pressure. Recovery from blackout occurs quickly on restoration of blood pressure. The presence of conscious function in the absence of vision can furnish pilots with a valuable warning that loss of consciousness is imminent unless appropriate steps are taken. Because of the repeatability of these symptoms, research studies often rely on subject reports of visual impairment as a measure of tolerance to +G<sub>z</sub>.

### Almost Loss of Consciousness

With increasing +G<sub>z</sub>, symptoms of early cognitive impairment can develop. This syndrome, termed *almost loss of consciousness* (A-LOC), consists of a transient incapacitation without complete loss of consciousness that often occurs during and after relatively short-duration, rapid-onset +G<sub>z</sub> pulses. A-LOC is characterized by a blank facial expression, twitching, hearing loss, transient paralysis, amnesia, poor word formation, and disorientation (14). The most prevalent symptom is reported to be a disconnection between cognition and the ability to act. The duration of incapacitation is much shorter than with G-induced loss of consciousness (G-LOC), reflecting a more transient degree of brain cell ischemia.

### G-Induced Loss of Consciousness

If cerebral hypotension progresses beyond the symptoms of visual impairment and A-LOC, G-LOC can occur. G-LOC has been defined as a “state of altered perception wherein (one’s) awareness of reality is absent as a result of sudden, critical reduction of cerebral blood circulation caused by increased G force.” (15) Centrifuge subjects who experience G-LOC frequently appear to stare blankly

before relaxing voluntary muscular control and exhibiting signs of loss of consciousness. Myoclonal jerking is often seen (approximately 70%), semipurposeful grasping and apparent efforts at reorientation are made, and amnesia is sometimes present with a complete unawareness that the event occurred. Following recovery from G-LOC, some subjects (and pilots in flight) have reported “dreamlets” that are similar to sleep dreams, except that they are of very short duration.

G-LOC incapacitation (after reduction of +G<sub>z</sub>) has been divided into two periods: absolute incapacitation (or unconsciousness) and relative incapacitation. According to centrifuge studies, the average absolute incapacitation period lasts 12 seconds (range of 2 to 38 seconds). This is followed by a period of relative incapacitation consisting of confusion/disorientation that lasts an average of 15 seconds (range of 2 to 97 seconds). A pilot is unable to maintain aircraft control during either of these periods, the sum of which is the total incapacitation period, averaging 28 seconds (range of 9 to 110 seconds). There is apparently no permanent residual pathological effect from an uncomplicated G-LOC.

If rates of onset of +G<sub>z</sub> are high, G-LOC can occur before other symptoms, including visual manifestations. Under these conditions, G-LOC can be rapid and lethal because it develops without warning. An example of this was documented several years ago through recovered telemetry data from a CF-18 Hornet jet aircraft. During an exercise combat engagement involving another aircraft, the pilot rapidly loaded the aircraft to +6.4 G<sub>z</sub>, then lost control within 4 seconds. The aircraft entered a near-vertical dive and crashed. The data indicated that 18 seconds after the loss of control an attempted recovery was made. The data demonstrated a total period of incapacitation of 18 seconds. The pilot was then able to recognize his situation and attempt recovery—unfortunately too late. Figure 4-9 is a plot of the recorded data.

In practice, it is often difficult to distinguish between A-LOC and G-LOC events. The symptoms and timing overlap, and form more of a continuum than two distinct syndromes. However, both historical and current literature assumes or portrays a clear difference.

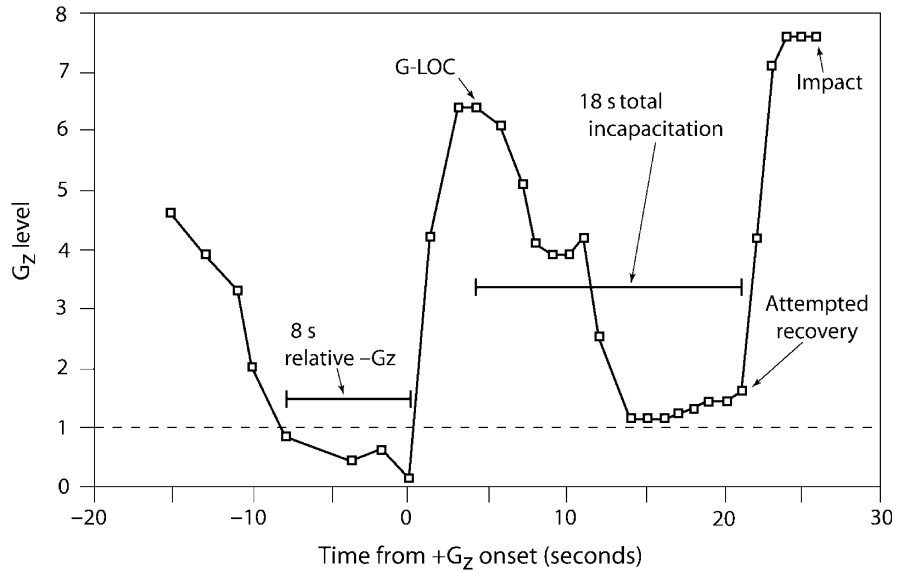
## Human Tolerance to Sustained +G<sub>z</sub>

Human tolerance to +G<sub>z</sub> has been studied on ground-based centrifuges using human volunteers. Objective measures of tolerance in the past have included ear pulse opacity, direct and indirect measures of blood pressure, and loss of consciousness. A less objective, but more widely used measure, consists of subject reports of visual changes. Unfortunately, reporting is variable and may be influenced by psychological or social pressures, anatomy, and slowed mental processing.

Human tolerance to +G<sub>z</sub> is influenced by many variables, including anthropometry (heart-to-brain distance), muscle straining, anti-G suit inflation, and rate of +G<sub>z</sub> onset. To control against some of these factors, standardized



**FIGURE 4-9** CF-18 Hornet crash data. These data were recorded during the fatal crash of a CF-18 Hornet.  $G_z$  is depicted along the vertical axis whereas time (in seconds) is depicted on the horizontal axis. The plot demonstrates approximately 8 seconds of relative  $-G_z$ , followed by rapid onset to  $+6.4 G_z$  and G-LOC and loss of control. The next control input was made approximately 18 seconds later with a rapid onset increase to  $+7.4 G_z$ , too late to avoid the crash.



approaches have been developed. One is to determine the tolerance of relaxed subjects. This allows for  $+G_z$  tolerance to be reported without the confounding influences of muscle strain or anti-G suit inflation, and offers a means of determining passive psychophysiological compensatory responses. Slower  $G$ -onset levels allow for cardiovascular compensation to influence the measure. Faster  $G$ -onset levels measure tolerance before a full cardiovascular response occurs.

In general, two separate types of subject tests are used, as defined by  $G$ -onset rate: (i) rapid-onset rate (ROR) tests and (ii) gradual-onset rate (GOR) tests. ROR is defined as a rate greater than 0.33  $G/s$ , often as high as 6  $G/s$ . GOR is defined as slower than 0.25  $G/s$ . Measurements of relaxed ROR  $+G_z$  tolerance are approximately 1  $G$  lower than GOR tolerances. The results of a study involving 1,000 relaxed male subjects reported tolerances presented in Table 4-2A (16). The results of World War II era centrifuge studies, based on subjective reports with onset rates of 2  $G/s$ , are also presented in Table 4-2B (17).

Researchers have studied other potential influences on human tolerance to  $+G_z$ . Studies assessing female relaxed

tolerance to  $+G_z$  concluded that they are equivalent to males, with reported ROR tolerances of  $4.2 \pm 0.5 G$  and GOR tolerances of  $5.2 \pm 0.6 G$  (18). Female time-to-fatigue during simulated air combat maneuvers is not significantly different from that for males (19,20). Menstruation in women on oral contraception has no effect on  $+G_z$  tolerance (19). Motion sickness lowers  $+G_z$  tolerance (21).

**Relative Negative Vertical Acceleration and Negative Acceleration ( $-G_z$ )**

In response to increased relative  $-G_z$ , heart rate is reduced and generalized vasodilatation occurs, a response that is relatively rapid. This response is dose related in the sense that increased relative  $-G_z$ , moving toward zero- $G$  and then  $-G_z$ , results in increasing blood pressure in the upper body and a more vigorous parasympathetic response (10).

During  $-G_z$ , intracerebral blood pressure increases. Congestion of the face and a subjective sensation of eye bulging occurs; this can become intense with increasing  $-G_z$ . There is upward movement of the abdominal contents and

**TABLE 4-2A**

**G-level Tolerances of 1,000 Relaxed Subjects Not Wearing Anti-G suits at 1 G/s Onset Rate**

Criteria	Mean G	± SD	G Range
PLL	4.1	0.7	2.2–7.1
Blackout	4.8	0.8	2.7–7.8
Unconsciousness	5.4	0.9	3.0–8.4

PLL, peripheral light loss.

(Source: Cochran LB, Gard PW, Norsworthy ME. *Variations in human G tolerance to positive acceleration*. USN SAM/NASA/NM 001–059.020.10. Pensacola, 1954.)

**TABLE 4-2B**

**G-level Tolerances of 300 Relaxed Subjects Not Wearing Anti-G Suits at 2 G/s Onset Rate**

Criteria	Mean G	±1 SD
PLL	3.5	0.6
Blackout	4.0	0.6
Unconsciousness	4.5	0.6

PLL, peripheral light loss.

Source: (Code CF, Wood EH, Lambert EH, et al. Interim progress reports and concluding summary of 1942–46 acceleration physiology studies. In: Wood EH, ed. *Evolution of anti-G suits and their limitations, and alternative methods for avoidance of G-induced loss of consciousness*. Rochester: Mayo Foundation Special Purpose Processor Development Group, 1990:409–430.)

the work of breathing is increased. Inverted flight ( $-1 G_z$ ) can be unpleasant, but tolerable. Between  $-2$  and  $-3 G_z$ , there is severe facial congestion and occasional reddening of vision. Most subjects can tolerate  $-3 G_z$  for 5 seconds, although some can reach  $-5 G_z$  without injury (10,22). The feeling of facial congestion becomes intense at  $-3$  to  $-4.5 G_z$ . The restraints, which are supporting the entire mass of the body, cause additional painful sensations. Competitive aerobic pilots describe sustaining up to  $-9 G_z$  for very brief durations.

Some of the adverse effects of  $-G_z$  derive from increased arterial blood pressure in the head, especially where it is unopposed. Within the skull, where increased arterial pressures are balanced by increased pressures in the surrounding cerebrospinal fluid, adverse effects are generally not seen (23). Where increased pressures are unopposed, injury can occur. Facial petechiae have been described by competitive airshow pilots. Nose bleeds and subconjunctival hemorrhage have been reported due to high  $-G_z$ .

There are no generally accepted countermeasures to  $-G_z$ , although some aerobic pilots report that they relax while exposed to  $-G_z$  so as not to further increase thoracic pressure.

### The Push-Pull Effect

Straight and level flying occurs at  $+1 G_z$ . A pilot experiencing relative  $-G_z$  or  $-G_z$  will be in a state of enhanced parasympathetic tone after several seconds of exposure. As a result, the pilot will experience bradycardia, diminished cardiac contractility, and vasodilatation.

If the pilot then flies a maneuver involving greater than  $+1 G_z$ , the upper body blood volume shifts forward into the increased intravascular space caused by vasodilatation. The fall in head-level blood pressure can be profound

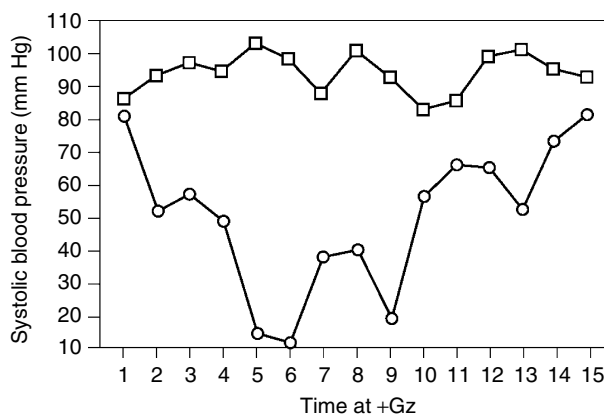


**FIGURE 4-10** These blood pressure data were recorded during a centrifuge experiment with a rate of onset of  $1 G/s$ . The upper plot shows the subject's systolic blood pressure response to  $+2.25 G_z$  following exposure to  $+1 G_z$ . In the lower plots, the same subject's response to  $+2.25 G_z$  is shown following pre-exposure to  $-1 G_z$ . Note the profound fall in blood pressure in the lower plot. The subject reported symptoms of grey-out, although G-LOC did not occur.

(Figure 4-10). Recall that the heart was initially in a state of bradycardia and low contractility. In this condition, a full compensatory response can take at least 8 to 10 seconds, with the recovery period dependent on both magnitude of  $-G_z$  and duration at  $-G_z$  (24–26). Given that the period of hypoxia latency for brain cells is only 4 to 6 seconds, the potential for  $+G_z$  related symptoms is clearly enhanced at lower than expected  $+G_z$  tolerance levels. Figure 4-10 demonstrates the blood pressure responses of a subject exposed first to  $+2.25 G_z$  following  $+1 G_z$ , then  $+2.25 G_z$  following  $-1 G_z$ .

The term *push-pull effect* (which describes the control stick input necessary to cause it) was coined to describe this phenomenon (9). It has been subsequently demonstrated in many studies involving humans and animals, and was demonstrated in humans during in-flight experiments (27).

### Transverse Acceleration ( $G_x$ )

When acceleration acts transversely, the vertical component of the hydrostatic fluid column is very short, and the location of the brain relative to the vertical column does not make the brain vulnerable to changing hydrostatic blood pressures. Predictably, centrifuge studies have demonstrated that the cardiovascular effects of  $+G_x$  are less than with  $+G_z$ . Negative  $G_x$  cardiovascular effects are generally similar to those of  $+G_x$ . If the head is elevated during  $+G_x$  exposures, heart rate increases, indicating some baroreceptor effect.

There is, however, considerable difference between  $+G_x$  and  $-G_x$  with regard to lung volumes and ventilation. At  $+6 G_x$ , for example, vital capacity is reduced 55% to 80% over  $1 G$  values, whereas at  $-6 G_x$ , there is only a minor decrease in vital capacity (28). Lung perfusion during  $+G_x$ , much like  $+G_z$ , is unevenly distributed within the lung: there is increased blood volume (shunting from right to left) near the back of the lung and no perfusion at the front. One minute at  $-6 G_x$  results in no reduction in arterial saturation.

Breathing effort increases during increased  $+G_x$  and, with reduced functional lung volumes, a higher breathing frequency occurs with an increase in functional dead space. The increased breathing effort during  $+G_x$  is caused by a major increase in the elastic component of the lung, with the total breathing effort doubled at  $+4 G_x$  over  $1 G$  (29). Oxygen consumption increases. Acceleration atelectasis occurs at  $+5.6$  to  $-6.4 G_x$  in subjects breathing 100% oxygen and not wearing an anti-G suit. Because lung volumes are not restricted during  $-G_x$ , acceleration atelectasis is not a problem. At higher  $+G_x$  levels, the inability of the subject to expand the chest wall upward (breathe) against the  $+G_x$  force limits human tolerance to approximately  $+15 G_x$  (30).

Despite the increased ability of humans to tolerate  $+G_x$ , this position has not been used as an anti-G system in high-performance aircraft. However, National Aeronautics and Space Administration (NASA) and Soviet spacecraft have employed the  $+G_x$  configuration to protect astronauts from high-G exposures during launch. This configuration is also used during entry of manned capsules, although the returning space shuttle exposes astronauts to predominantly  $+G_z$  (Table 4-5) (31).

## Lateral Acceleration ( $G_y$ )

The brain is also not directly threatened during  $G_y$  because of the relatively short vertical hydrostatic column that exists in this orientation.  $G_y$  is rarely encountered in current aircraft. It may become an important concern in future aircraft capable of lateral thrust-vectoring propulsion (TVP). The most important physiological problem involving lateral acceleration up to  $\pm 6 G_y$  is dyspnea as a result of ventilation/perfusion inequalities. Radiologic images demonstrate marked displacements of the heart and compression of lung toward the acting forces (32). Research involving  $G_y$  has demonstrated reductions in blood oxygen saturation levels starting 10 to 15 seconds after the onset of  $G_y$ . This trend is worse for  $+G_y$  compared to  $-G_y$ , and neck discomfort is problematic beyond 3  $G_y$  (33).

## Multiaxis Acceleration

Multiaxis accelerations can occur during flight maneuvers involving thrust-vectoring aircraft such as the United States Air Force (USAF) F/A-22 or the Russian Su-37, and can either enhance or reduce relaxed tolerance to the  $+G_z$  component of acceleration. Simultaneous  $G_y$  and  $G_z$  enhance  $+G_z$  tolerance, whereas simultaneous  $G_x$  and  $G_z$  can reduce  $+G_z$  tolerance. These differences are small and unlikely to affect operations (34).

## Morbidity and Mortality

The overall incidence of in-flight G-LOC among military aircrew during their careers is between 8% and 25% (35–37), levels that have remained steady over the last 20 years. Reported G-LOC incident rates for trainer, attack, and fighter aircraft average 25.2 events per million sorties (PMS). However these rates range from 1.4 G-LOCs PMS for two-crewmember fighters to 112.4 PMS for basic trainers (37). Most such incidents occur during training flights, and usually affected aircrew who were not in control of the aircraft when their G-LOC occurred (35), a factor that prevented crashes. Although centrifuge training programs have been associated with decreased reports of in-flight G-LOC, reduced incidence of in-flight G-LOC was not noted among USAF pilots in the 1990s (38). Inexperienced pilots report more incidents of G-LOC (38).

Mission type rather than aircraft type influences the G-LOC incidence. The G-LOC rate in the USAF by aircraft category is reported in Table 4-3 (37). For a variety of reasons, including amnesia of the event, self-reports of in-flight G-LOC are certainly underestimated.

The push-pull effect has been implicated as an important cause of G-LOC in flight. A recent Royal Air Force (RAF) study reported that approximately 31% of in-flight G-LOC was due to push-pull effect, similar to the 29% reported in a separate study conducted by the USAF (35,39). Push-pull effect-like maneuvers were previously reported as a problem in competitive aerobatic flying (40). Although the push-pull effect is most applicable to trainer, fighter, and civilian aerobatic aircraft, the flight envelopes of modern helicopters

TABLE 4 - 3

### United States Air Force (USAF) G-induced Loss of Consciousness (G-LOC) Event Rates by Aircraft Category (1982–2002)

Aircraft	Sorties	Events (Rate <sup>a</sup> )	Expected Events
Single crewmember fighters	7,640,702	83 (10.9)	193
Two-crewmember fighters	2,919,320	4 (1.4)	74
Attack	2,784,219	5 (1.8)	70
Basic trainers	4,091,059	460 (112.4)	103
Advanced trainers	4,631,538	6 (1.3)	117
Total	22,066,838	558 (25.2)	

<sup>a</sup>Per million sorties (PMS).

(Source: Lyons TJ, Craft NO, Copley GB, et al. Analysis of mission and aircraft factors in G-induced loss of consciousness in the USAF: 1982-2002. *Aviat Space Environ Med* 2004;75: 479–482.)

give rise to the possibility that A-LOC can occur during aggressive flight operations (41).

The identification of G-LOC as a causal factor in crashes is complicated by the lack of data and survivor information that accompany such events. Crashes due to suspected G-LOC are usually fatal and involve single-pilot aircraft. Overall, in the USAF, 20 fatalities have been caused by G-LOC in recent years (37). A Canadian CF-18 was lost due to G-LOC during an air combat training exercise in 1995 and push-pull effect was found to be causal (Figure 4-9). The loss of an F-20A Prototype Tigershark in Canada in 1987 was also attributed to G-LOC by the investigating board. A case of G-LOC has been reported in general aviation (42).

## Protection Against the Effects of $+G_z$

Protection against the effects of  $+G_z$  can be approached through several means, including: (i) decreasing the vertical heart-to-brain distance, (ii) limiting duration to less than 4 to 6 seconds, (iii) increasing blood pressure at the aortic valve, and (iv) avoiding the push-pull effect.

### Decrease Heart-to-Brain Distance

The most effective means of enhancing  $+G_z$  tolerance, as well as protecting the pilot, is to reduce the vertical height of the heart-to-brain distance. This reduction can be made possible by having the subject tilt either forward (prone) or backward (supine) relative to the  $+G_z$  vector. The approach has been used in the design of modern fighters including the F-16. The heart-to-brain distance can also be reduced by the presence of an anti-G suit (by elevating the diaphragm).

### Limit Duration

Civilian competitive aerobatics pilots, who do not use anti-G suits, report experiencing up to  $+12 G_z$  and levels of  $-G_z$  approaching  $-9 G_z$ . Because many such pilots perform sustained inverted flying maneuvers, susceptibility to the

push-pull effect is an acknowledged threat. However, due to aircraft thrust limitations, most competitive aerobatic aircraft are not capable of prolonged sustained  $G_z$ , and the pilots are able to tolerate these high levels because exposure times are less than 4 to 6 seconds.

### **Increase Aortic Valve Blood Pressure**

Any measure that safely increases aortic valve blood pressure, as a means of countering the increased hydrostatic component of blood pressure during increased  $+G_z$ , will enhance human tolerance. The most effective way of accomplishing this goal is by utilization of the anti-G strain maneuver (AGSM), first developed during World War II.

### **Anti-G Strain Maneuver**

The AGSM consists of forced exhalation against a closed glottis (L-1 maneuver) or partially closed glottis (M-1 maneuver) while tensing leg, arm, and abdominal muscles. The AGSM effort is interrupted at 3- to 4-second intervals with a rapid (<1 second) expiration/inspiration, which allows adequate venous return during the period of low intrathoracic pressure. Although head-level blood pressure falls to nearly zero in conjunction with lowered thoracic pressure, the time is so brief that the brain maintains unaltered function.

Tensing increases intrathoracic pressure, which is directly transferred to arterial pressure at heart level. With increased  $+G_z$ , and despite cardiovascular compensation, cardiac output decreases because of the reduced stroke volume as a consequence of the fall in venous return (43). Muscular tensing of the legs is used to increase vascular resistance to assist venous return.

The AGSM technique is learned. An effective teaching platform is formal AGSM training on a human-use centrifuge. Training that includes simulated air combat has proved effective in enhancing tolerance. A well-trained and current pilot can raise  $+G_z$  tolerance by up to 3 G (44). One recent training program included push-pull effect maneuvers (45).

The AGSM is fatiguing. Physiological support for the AGSM is primarily anaerobic with muscular strength as a principal factor in its intensity. Both anaerobic capacity and muscular strength can be increased with training. Strength training has been shown to increase  $+G_z$ -duration tolerance. Suddenly ceasing to perform an AGSM, while still at elevated  $+G_z$ , predictably leads to G-LOC.

### **Anti-G Suits**

The anti-G suit (also termed *G-suit*) is designed to provide transient hypertension at the aortic valve to overcome hydrostatic pressure. Two general approaches to the design of anti-G suits have been taken: hydrostatic and pneumatic. Hydrostatic anti-G suits use fluid within the suit to provide counterpressure to the body simultaneously with  $+G_z$  stress. These suits are self-contained, require no aircraft support or attachments, and provide an instant response. The first operationally deployed anti-G suit used this principle (7).



**FIGURE 4-11** On the left is a conventional anti-G suit used during World War II. On the right is a modern anti-G suit used in the CF-18 Hornet. Note the small change in the basic design over 50 years.

It was soon abandoned in favor of the lighter and more comfortable pneumatic designs, but the modern Libelle suit has signaled a return to this concept. Figure 4-11 consists of a photograph of a conventional anti-G suit that was used operationally in World War II and a photograph of a modern conventional anti-G suit.

The pneumatic anti-G suit generally consists of pressure bladders inside fabric coveralls that cover the abdomen, thighs, and calves. Air pressure is supplied to the bladders through control valves at rates that depend on the level of  $+G_z$ . The suits are designed to be tightly fitted with zipper fasteners and air hose connectors that attach to the aircraft. Successfully developed in World War II in several versions, the design evolved after the war to include less body surface coverage for increased comfort. With the advent of aircraft capable of higher and more sustained  $+G_z$ , designs reverted to the enhanced body coverage of the earlier era.

Conventional anti-G suits increase aortic valve blood pressure by (i) increasing total peripheral resistance through mechanical compression of the abdomen and legs, (ii) raising the position of the heart to decrease the vertical distance to the brain, and (iii) increasing venous return. Optimum response time for suit inflation is within 1 second of reaching the maximum  $+G_z$  level. The effectiveness of an anti-G suit depends on the amount of pressure applied (and tolerated) to the abdomen and trunk, the area of application, and the volume of the bladders. In general, highest protection is afforded at the highest tolerable pressure, and depends on the subject and suit fit.

A conventional anti-G suit increases relaxed ROR and GOR tolerances by approximately 1 to 1.5 G. Protection is dependent on a properly tight fit with all “comfort zippers” worn and closed. The USAF Advanced Tactical Anti-G Suit (ATAGS), a suit that covers a greater portion of the legs and abdomen, increases G-tolerance by an additional 0.5 to 1.0 G. The protective qualities of the anti-G suit are generally considered additive to the protection afforded by the AGSM.

Therefore, a pilot who has a resting tolerance of  $+5 G_z$  would be expected to tolerate up to  $+9$  to  $+10 G_z$  with a properly functioning anti-G suit and a well-performed AGSM.

To prevent fatigue during air combat maneuvering, assisted positive pressure breathing for G (PBG) was developed. The concept works by increasing mask pressure during  $+G_z$  with the result that pilots must exhale forcefully. Inspiration is also assisted and augmented. The increased inspiratory pressure, and forced exhalation, increases intrathoracic pressure and thereby aortic valve blood pressure.

An example of this technology is the USAF version of PBG, the COMBAT EDGE. COMBAT EDGE uses a chest-counterpressure garment (jerkin) that is worn and inflated at the same pressure as the breathing mask delivering the increased intrapulmonary pressure. This jerkin counteracts high levels of positive pressure breathing by supporting the chest. Research has explored whether the counter pressure jerkin is necessary for PBG under all circumstances. A counter pressure jerkin is necessary when positive pressure is utilized for altitude protection, but the increased weight of the chest when a pilot is exposed to G may provide sufficient counter pressure for PBG in other conditions.

PBG reduces the fatigue that develops during high-G maneuvers, because the requirement to perform an AGSM is reduced by approximately 50%. The PBG/ATAGS combination and reclined seatback offers high-G protection that will allow many pilots to tolerate  $+9 G_z$  sustained with minimal or no AGSM (13). This type of design is currently in use in the F-22, Typhoon, Finnish F-18, and Norwegian F-16. Significant benefits have been reported by pilots using these suits. Studies of the full-coverage PBG concept report that trained subjects can tolerate five simulated flight sorties over 4 hours with up to 80 peaks to  $+9 G_z$  and 80 peaks to  $+8 G_z$  (46).

### Avoiding the Push–Pull Effect

Apart from efforts to inform pilots of the hazards of the push–pull effect, no countermeasures against the problem have yet been developed.

### Potential Harmful Effects of Sustained G

In general, exposure to  $G_z$  within the acceleration capabilities of current aircraft does not lead to permanent injury. Most reported injuries are minor and consist of neck strains. No permanent sequelae to centrifuge G-LOC, even when repeated, have been reported.

Although animal studies have demonstrated myocardial injury from tolerable levels of increased  $+G_z$ , these results are not considered applicable to humans. No pathologic changes were detected during the autopsy of a highly exposed centrifuge subject (47). A cross-sectional study found no differences in right and left ventricular dimensions and wall thickness, aortic and left atrial dimensions, and tricuspid and mitral inflow velocities of pilots compared to nonpilots (48).

Cardiac dysrhythmias, usually benign, have been documented during centrifuge studies. These dysrhythmias are

generally considered to be due to changes in the electrical mechanism of the heart. Seldom are there symptoms of compromise to  $+G_z$  tolerance. The incidence of in-flight dysrhythmias may be lower than the reported incidence derived from centrifuge experiments. No clinically significant in-flight dysrhythmias have been recorded.

Acceleration (or aero-) atelectasis syndrome is associated with increased  $+G_z$  exposure in pilots who breathe oxygen-enriched gas mixtures ( $>70\%$  oxygen) and wear an inflated anti-G suit. Symptoms include retrosternal chest pain or discomfort, dyspnea, and episodes of paroxysmal coughing. This condition occurs because the downward movement of the lung is opposed by the upward shift of the diaphragm caused by inflation of the abdominal bladder of the anti-G suit, thereby compressing lower lung tissue and closing the distal alveolae. Oxygen in these isolated alveolae is rapidly absorbed into the blood, resulting in their collapse. Not surprisingly, breathing oxygen can contribute to acceleration atelectasis (49). There is a high degree of individual susceptibility to acceleration atelectasis, which may be increased by tobacco smoking.

Movement of viscera due to  $G_z$  is known to occur, but reports of associated injuries are rare. The heart is known to move within the thorax and relative to the diaphragm under  $G_z$  loading. There has been a single report of renal artery dissection as a result of visceral movement during  $\pm G_z$  (50), and one occurrence of acute inguinal hernia thought to be associated with the AGSM (51).

Musculoskeletal symptoms are probably the most common complaints associated with  $+G_z$ . Neck pain is often associated with extremely rapid-onset  $+G_z$  during aerial combat or aerobatics, usually when the neck is near maximum rotation. The risk of neck injury may be associated with a reclined seat and the presence of a helmet. Although radiologic studies conducted at up to  $+6 G_z$  have shown no measurable narrowing of intervertebral spaces (17), some consider degenerative conditions likely as a result of repeated overloading of vertebrae. A recent study using magnetic resonance imaging (MRI) did not find a high prevalence of cervical degeneration changes among a small number of fighter pilots (52).

Pain is sometimes reported in dependent areas subject to venous congestion, especially with use of full coverage anti-G suits. These complaints include reports of arm pain that has been treated successfully with inflatable arm cuffs. Also found in dependent and unsupported areas of the body are small, pinpoint, cutaneous petechiae (previously discussed), often called *G-measles* or *Geasles*. They resolve in several days without sequelae. Occasional problems with larger vessels have been reported, including superficial lower extremity phlebitis and hematomas, and there is an anecdotal belief among pilots of an increased incidence of hemorrhoids.

### The Limitations of Current Knowledge

In the past, human tolerance to increased  $+G_z$  was associated with magnitude, duration, rate of onset, use of

countermeasures, and individual susceptibility. Pre-exposure  $G_z$ -history (e.g., the push-pull effect) was not considered a risk factor to reduced  $+G_z$  tolerance.

Human centrifuges usually consist of a capsule (or gondola) mounted at the extremity of a rotating arm.  $G$  varies with the distance from the center of rotation and with the velocity of the capsule according to Equation 4. The capsule is usually attached to the end of the rotating arm in a manner that allows it to roll passively into alignment with the resultant  $G$ -vector, which is the vector addition of rotational- $G$  and gravity. An upright-seated occupant inside the capsule then experiences  $+G_z$ .

All human centrifuges create accelerations greater than  $+1 G_z$ . To create other directions of  $G$ , the capsule, or the occupant and seat, are mechanically rotated out of alignment with the resultant  $G$ -vector. For example,  $-G_z$  can be produced if the centrifuge subject is inverted within the capsule so that the subject is “head-out” from the center of rotation.  $G_x$  and  $G_y$  are achieved when the subject is presented transverse to the resultant  $G$ -vector. In the past, most centrifuges did not have this capability or were unable to change acceleration directions during rotation. Less than half of present-day centrifuges have this capability.

Another limitation of centrifuges is the need to mitigate the potentially disorienting cross-coupled effects on the inner ear of the centrifuge subject. This is accomplished by starting slowly and gradually increasing the rotational velocity of the centrifuge until a “baseline” condition is achieved. The baseline, which typically varies from  $+1.2$  to  $+1.8 G_z$ , represents the starting level.

These situations contrast with actual flight conditions. Figure 4-12 depicts the accelerations recorded during two F/A-18 sorties (53). Note that 5% to 6% of flight time during these sorties was conducted at less than  $+1 G_z$ , with even more time spent at less than  $+1.2$  to  $+1.8 G_z$ . Figure 4-9 demonstrated the acceleration profile of a fatal CF-18 crash. Immediately preceding the loss of control, the pilot experienced relative  $-G_z$ , which led to  $G$ -LOC.

In a separate study of 240 USAF air combat engagements, it was found that up to 67% of engagements included maneuvers that could provide the push-pull effect (54). Table 4-4 illustrates the incidents.

The great majority of the thousands of studies involving acceleration research during and after World War II occurred at levels greater than  $+1 G_z$ . The variable of preceding  $G_z$ -history was not considered. The experimental conditions, for the most part, were imposed by the capabilities of the centrifuges and the lack of appreciation of the potential role of preceding  $G_z$ . The variable of preceding occupant  $G_z$ -history has therefore not been widely considered in the design of countermeasures, including anti- $G$  suits.

## The Future

Current and future crewed fighter aircraft will employ TVP, which is the redirection of engine thrust in flight (55). TVP

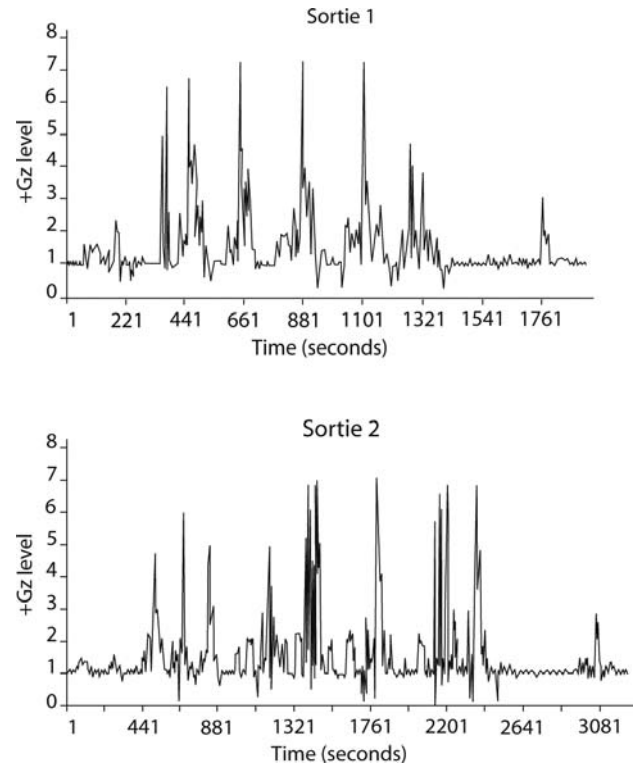


**FIGURE 4-12** Two F-18 flight profiles recorded during air combat maneuvering.

enables “high-agility” maneuvering, which is the capability of an aircraft to maintain controlled flight at speeds below that of the airframe stall speed. Current aircraft employing aspects of this technology include the Lockheed Martin F-22, versions of the F-15, F-16, F-18, the Mikoyan-Gurevich MiG 35 MFI, Sukhoi Su-37, and the Su-47.

The tactical advantages of high-agility flight include improved capabilities in “point-first” missile attack, ground

**TABLE 4 - 4**

### Percentage of Engagements with Push-Pull Effect Maneuvers by Type of Sortie, Pilot Status, and Aircraft Type

Sortie Type	Pilot Status	Aircraft		Combined (%)
		F-16	F-15	
BFM	Student	11/30(37%)	7/43(16%)	25
BFM	Instructor	3/28(11%)	5/35(14%)	13
ACM	Student	18/42(43%)	16/24(67%)	51
ACM	Instructor	12/32(38%)	5/8(63%)	43
Aircraft totals		44/132(33%)	33/110(30%)	132

BFM, basic fighter maneuvers; ACM, air combat maneuvers.

(Source: Michaud V, Lyons T, Hansen C. Frequency of the “push-pull effect” in U.S. Air Force fighter operations. *Aviat Space Environ Med* 1998;69:1083-1086.)

attack, reconnaissance, missile avoidance, high-altitude operations, short take-off and landing, automaneuvering, stealth, and safety. Flight maneuvers, such as the Herbst and Cobra maneuvers, have evolved. It is expected that  $+G_z$  exposure magnitudes in the future will be of lower magnitude, but increased frequency. Negative- $G_z$  exposures will be more frequent.  $G_y$  exposures, now rarely experienced, will become more common and  $G_x$  stress will increase in magnitude with improvements in propulsion systems (55).

A knowledge gap exists. Current  $+G_z$  countermeasures, including anti-G suit technology, provide inadequate protection against the stresses of high-agility flight. Pneumatic or hydraulic anti-G suit technology that responds quickly to the array of internal hydrostatic pressure challenges will be needed. Hopefully, individualized closed-loop algorithm-based systems, that incorporate the variable of preceding  $G_z$ -history, will be developed.

Thirteen years after the identification of push-pull effect, and 10 years after it was first identified as causal to upward of 30% of G-LOC incidents, an effective countermeasure has yet to be devised.

## Space Operations

Space vehicle launch and entry involve significant accelerations. Table 4-5 summarizes some of the accelerations experienced during manned spaceflight (31).

In order to tolerate these accelerations, astronauts are orientated to experience  $+G_x$  both before and during launch (Figure 4-13). Space capsule seating has involved rigid contoured seats, while seating within the Space Transportation System (STS) space shuttle crew module consists of up to seven conventionally aligned seats, five of which are removable during flight. The seats are rigid in construction, fastened to floor structures, and equipped with conventional five-point restraint harnesses. Personal life-support equipment includes full pressure suits with helmets,

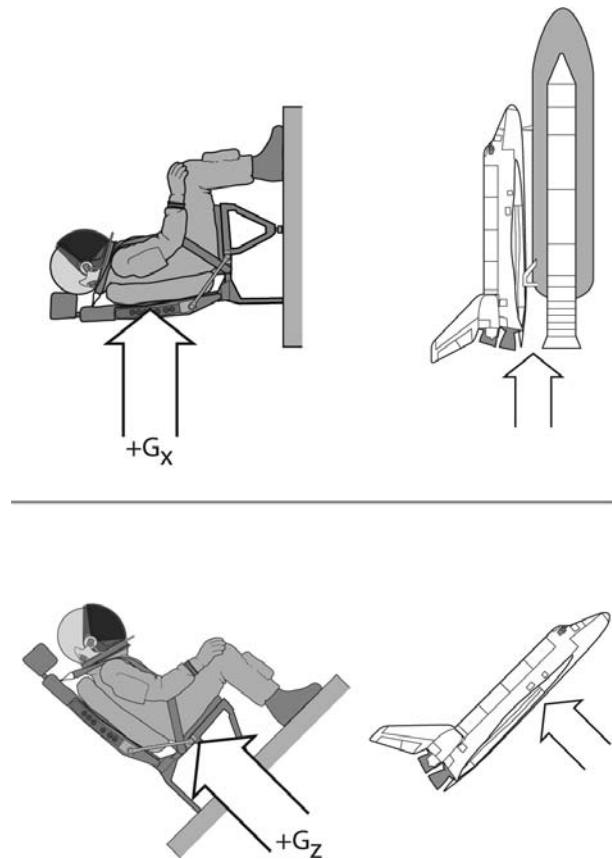


**FIGURE 4-13** The top diagram depicts the orientation of astronauts before and during launch of the space shuttle and Soyuz. In this orientation, they experience  $+G_x$  during launch. In the lower depiction, the orientation of space shuttle astronauts during entry is shown. While encountering increased atmospheric drag, the crew experiences predominantly  $+G_z$ . (Source: John Martini, BRC).

detachable gloves, boots, and parachutes. The space shuttle does not have ejection seats and emergency escape is through a bailout procedure.

Because the space shuttle is vertically aligned to the Earth before launch, seated astronauts experience  $+1G_x$  (gravity). As acceleration builds during the climb-out from the Earth,  $+G_x$  stress increases to approximately  $+3 G_x$ . Positive- $G_x$  is best tolerated because the hydrostatic column is aligned in a manner that does not directly threaten intracerebral function, but the work of breathing is increased (as described previously).

Once orbital insertion has occurred, astronauts begin a freefall and experience no G due to gravity. In aerospace medicine, this is termed *microgravity*. During a suborbital launch into space (Space Ship One), zero-G is experienced for a short period, but the spacecraft soon falls to Earth.

In microgravity, there is no hydrostatic blood pressure component and all blood pressure is due to the dynamic component, which is undiminished at head level. Leg volume decreases and facial soft tissues expand. There are initial increases in the size of the heart, and cardiac

**TABLE 4-5**

### Spacecraft Launch and Entry Acceleration Profiles

Vehicle	Launch Profile	Reentry Profile (Average Max G)
Mercury-Atlas	6.0G for 35 s and 6.4G for 54 s in two phases over 6 min with peaks of 8.0G	8.9G (range 7.6–11.1G)
Voskhod		3.0–4.0G
Gemini-Atlas	Peaks of 5.5G and 7.2G	5.7G (range 4.3–7.7G)
Soyuz	3.4–4.0G	3.0–4.0G
Apollo-Saturn	Little >4.0G	5.9G (range 3.3–7.2G) for up to 60 s.
Space Shuttle	3.4G	1.2G for 17 min

output and stroke volume are increased. Cardiopulmonary receptors, which function to control blood volume on Earth, stimulate adaptive mechanisms aimed at reducing blood volume. Plasma volume drops rapidly, probably through movement into the extravascular space (56). Blood volume is decreased, likely as a result of reduced erythropoietin secretion. With the overall reduction of physical activity in space, cardiac muscle mass is reduced (along with other muscles). Cardiac rhythm disturbances have been reported (56).

On return to Earth, manned space capsules enter the atmosphere in an attitude that again results in  $+G_x$  stress to the crew. The space shuttle attitude during entry leads to  $+G_z$  stress that averages  $+1.2 G_z$  for 17 minutes before touchdown (Table 4-5). The combination of muscle atrophy, reduced cardiac mass, and dehydration in the presence of significant fluid shifts, are preconditions for reduced  $+G_z$  tolerance during this phase. As part of entry procedures, shuttle astronauts rehydrate and wear anti-G suits with optional inflation levels. Normal procedures call for strap-in to be complete before entry-interface (first interaction with atmosphere). Since the loss of Challenger in 1986, all shuttle crews have been required to wear an anti-G suit during entry. Those who inflate the suits have better protection against  $+G_z$  during entry and landing (57).

### $+G_z$ Tolerance Models: A Need for a Revision

The most generally accepted model of  $+G_z$  tolerance was proposed by Alice Stoll in 1956 (58). This model was based on original experimental data, and was integrated with the results of similar experiments conducted in other laboratories. A G-tolerance curve that incorporated various acceleration rates was created. Other versions of this curve have been presented in previous editions of this book. The Stoll G-tolerance curve is reproduced in Figure 4-14.

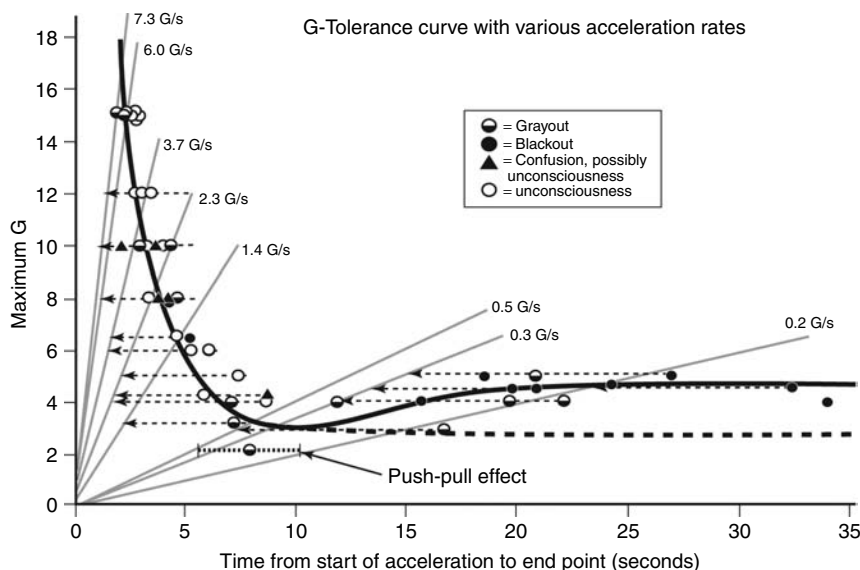


**FIGURE 4-14** Stoll  $+G_z$  tolerance curve. A line has been added to the plot to show a range of visual symptom reports among subjects pre-exposed to  $-1 G_z$  or  $-2 G_z$  (labeled the push-pull effect).

The Stoll curve was based on centrifuge studies and therefore describes the experiences of healthy young males exposed to accelerations greater than  $+1 G_z$ . Although it adequately describes the tolerances of subject populations involved in centrifuge research, the use of the Stoll plot (and other similarly derived models) should be viewed with caution when applied to operational conditions.

When pre-exposure  $G_z$ -history is considered, predictions based on the Stoll model will overestimate human tolerance. The extreme example involves space flight operations. As discussed previously, space flight leads to physical deconditioning and markedly reduced tolerance to  $+G_z$ , including the  $+1 G_z$  of gravity. Much shorter durations of zero-G, like those experienced during atmospheric ballistic flights to train astronauts, have led to symptoms of reduced  $+G_z$  tolerance during the moderate  $+G_z$  of aircraft recovery. To illustrate the problem, we have added a line to the Stoll plot in Figure 4-14 showing reports of visual light loss from subjects exposed to  $+2.25 G_z$  after the preceding  $-G_z$  (24). The line falls below the predicted tolerance predicted in the Stoll curve.

When considering pre-exposure  $G_z$ -history, both magnitude and duration of  $G_z$ , two separate but associated variables must be considered. Modeling, based in part on the Stoll data, has aimed at predicting the cognitive and blood pressure effects of these two variables on subsequent  $+G_z$  tolerance. This modeling demonstrates the inadequacies of Stoll-like predictive models when  $+G_z$ -history is considered (59).

A revised model is needed, particularly in light of ongoing progress toward space tourism and the likelihood that pilots and passengers of commercial space vehicles will be exposed to stresses of flight that are, as yet, incompletely understood. The variable of pre-exposure  $G_z$ -history is now added to the list of risk factors for G-LOC. The Stoll curve, long relied upon, should be viewed as an evolving, dynamic entity that varies with  $+G_z$ -history.



## TRANSIENT ACCELERATION

Transient acceleration is encountered by aircrew both in the course of flight operations and during emergencies. Operational exposures to transient acceleration include aircraft carrier catapult launches, barrier engagements, and capsule recovery impacts. Transient accelerations are also encountered during emergencies that involve ejection, parachute opening, and ground landings. Crashes involve very large and injurious levels of transient acceleration.

Transient and sustained accelerations are often delineated in terms of duration. For example, acceleration events having durations of less than 1 or 2 seconds have been defined as impacts by various authors. However, a fixed-time duration definition is not always applicable over the range of acceleration profiles of interest in aerospace medicine. Depending on how brief an impact duration is, the result on an aircrew member can range from little noticed to catastrophic. The injury outcome may provide the best way of considering the issue: traumatic injury is associated with transient acceleration; challenges to homeostasis are associated with sustained acceleration.

The designs of space vehicles, cockpit escape modules, ejection seats, parachutes, and restraint systems have been based on human tolerance data derived from research using volunteers, cadavers, and animals. This section begins with a brief review of the basic mechanics of transient acceleration, and then describes the current understanding of human tolerance. Emergency crew escape, crew protection, and aircraft crashes are then discussed.

### Work and Energy

One convenient way of understanding transient acceleration is through the concept of energy, which can be considered as the ability to do work. Kinetic energy is a form of energy that exists by virtue of motion. Kinetic energy is expressed as:

$$E = 1/2 mv^2 \quad [8]$$

where  $E$  = kinetic energy.

Kinetic energy is proportional to velocity squared and varies directly with mass. For example, a 6-mm diameter bolt in low-Earth orbit has about the same mass but 10 times the velocity of a military rifle bullet, and hence 100 times its energy.

With energy, work can be accomplished. A hammer strikes a nail and the nail is driven, against friction, a certain distance into a board. Assuming all the energy has gone into moving the nail into the board, the kinetic energy of the hammer was converted to work.

Work is defined as the product of force and distance, or:

$$W = Fx \quad [9]$$

where  $W$  = work and  $x$  = distance.

Of interest, the units of work and energy are the same, and, as a practical consequence, they are equivalent. If all of the kinetic energy of an impact event is used in work (an

assumption), it is possible to estimate the average acceleration of the event as follows:

$$E = W \text{ or } 1/2 mv^2 = Fx \quad [10]$$

which leads to:

$$a = v^2/2x. \quad [11]$$

When the acceleration is applied to an occupant who is perfectly fixed to the aircraft (another assumption), the  $G$  on the occupant can be expressed as:

$$G = v^2/2gx. \quad [12]$$

Consider the scenario of an aircraft in flight impacting the terrain. In the moment before impact, the aircraft possesses kinetic energy according to its velocity and mass (Equation 8). After striking the terrain and decelerating through a distance, the aircraft comes to rest and its kinetic energy is zero. This is depicted in Figure 4-15A. If we assume that all the kinetic energy is converted to work (for example, by destroying aircraft structures, or reacting to opposing forces), and we know the distance of the deceleration, we can estimate the *average*  $G$  of an occupant fixed to the aircraft by using Equation 12.

Note that in Figure 4-15B, the same example is presented, but the depicted distance of deceleration is much shorter than that of Figure 4-15A. If we again use Equation 12, the calculated average  $G$  would then be greater. The crash at Figure 4-15B is clearly the more severe in terms of occupant exposure to  $G$ , and the severity relates to the deceleration distance and velocity.

These estimates are based on a constant deceleration, which never occurs in a crash. Crash events are usually measured on a time scale of a few hundred milliseconds. Within this scale, deceleration (and associated crash forces) starts at zero, rise to a peak, and end at zero when the event is over. Therefore, the greatest acceleration, or “peak- $G$ ” is often of more interest. An estimate of peak- $G$  can be made by doubling the average estimate from Equation 12. When more information is available, a more robust analysis using nonconstant accelerations can sometimes be generated.

These very important concepts underlie all that will be discussed in this section. For the same velocity and mass, the acceleration experienced by an aircraft, and the  $G$  experienced by the occupant, depends (in part) on the distance of deceleration. Protection from injury is usually enhanced when the kinetic energy can be dissipated over a greater distance.

### Kinematics and Biomechanics

Kinematics involves the analysis of motion without reference to force. Biomechanics is the description of the effects of mechanics (force, energy, acceleration, momentum) on humans affected by transient acceleration. Descriptions of impact response usually involve the displacement of the subject with respect to the vehicle. One way in which displacement can increase occupant accelerations is by imposing shorter stopping distances for some parts of the body, a phenomenon seen during a crash landing. In such events, the initial velocity of the aircraft is rapidly decreased to zero relative to the terrain.

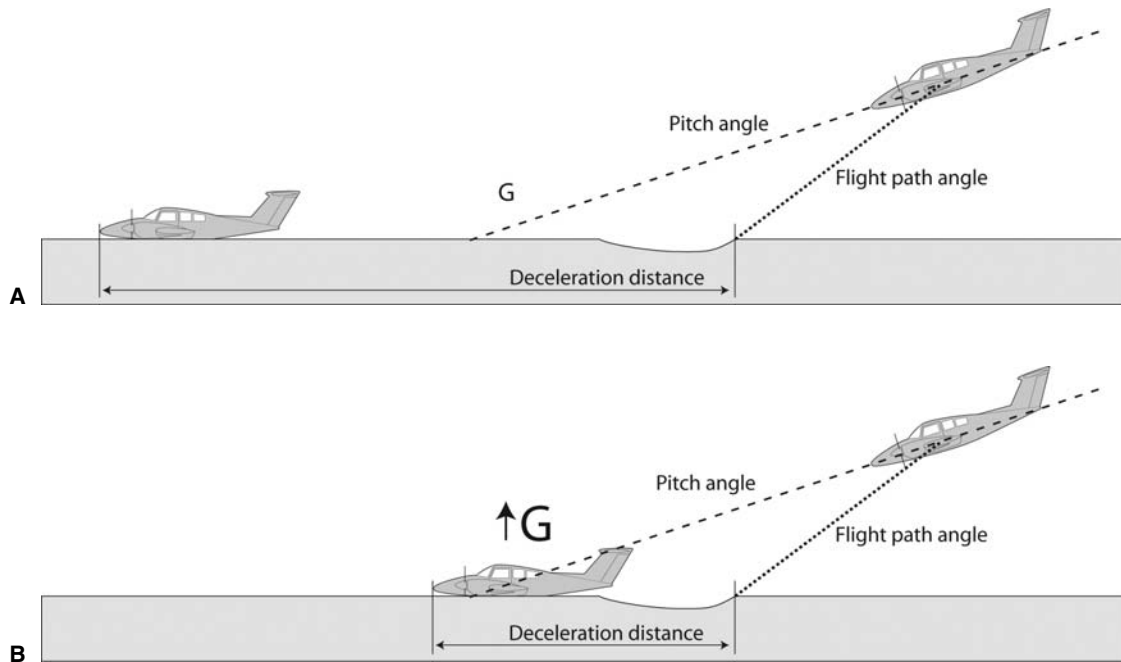


**FIGURE 4-15** **A:** Aircraft at rest following crash into terrain. The aircraft has impacted the terrain and translated to a stop. The total distance of deceleration is indicated. A resultant average deceleration is depicted with “G.” (Source: John Martini, BRC). **B:** This depiction shows the same aircraft, but with a much shorter stopping distance. Because the distance is shorter (and referring to Equation 12), the average “G” is greater. The associated forces and potential for injury would also be greater when compared to A (Source: John Martini, BRC).

For a human involved in a frontal crash, the head continues forward at the preimpact velocity until influenced by a force that acts to cause an acceleration. In this example, the force is provided by the neck that is ultimately placed in tension as the head continues forward with respect to the rest of the body (Figure 4-3). A velocity difference is therefore built up between the head and the body, because the latter is restrained by the straps of the restraint harness. The head will then have to undergo the same velocity change but in less time than the body because it starts to decelerate later: both the body and the head must finally reach zero velocity. Displacement of a pilot from a normal cockpit position may allow the pilot to strike a portion of the aircraft, such as the instrument panel. This leads to increased head accelerations.

The manner by which an occupant is coupled to contact surfaces influences their response to transient acceleration. For example, helmets act as buffers to increase the distance over which the head changes velocity. Restraint systems allow individuals to remain fixed to the aircraft while it decelerates through a crumpling crush zone. Ejection seat propellant cartridge catapults, and rockets ignited upon entering the wind stream, provide the acceleration necessary to escape from the aircraft.

Even when surfaces and equipment are optimally designed, human tolerance to the energy of transient acceleration has its pathophysiological limit. If designs are in place that can lower the G experienced by an occupant during a crash, protection against trauma can be afforded. Some

helicopters have stroking seats that help protect the spine during vertical impacts. The principle of stroking seats is to increase the distance of deceleration and thereby decrease the G experienced. This is illustrated in Figure 4-16.

By increasing the distance of deceleration of the pilot during the crash, forces are reduced and injury potential is lessened.

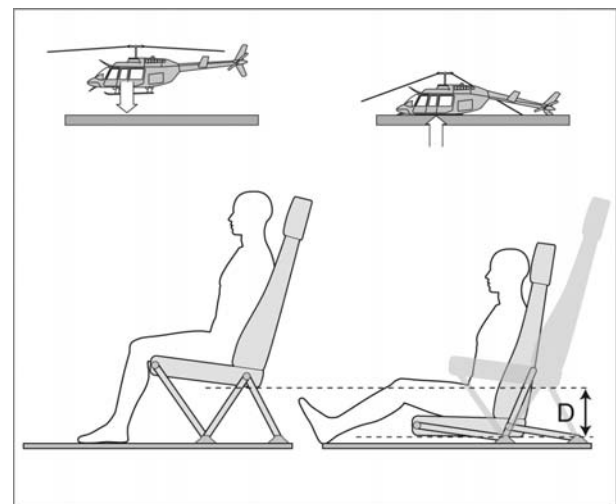


**FIGURE 4-16** The principle of stroking seats. A design that allows the seat to stroke downward in a vertical impact increases the distance of deceleration and reduces G and the potentially injurious forces acting on the spine (Source: John Martini, BRC).

## Tolerance and Tolerance Limits

In its simplest form, human tolerance can be defined as the “ability to endure” without harm, or with acceptable harm. Human tolerance to transient acceleration can be defined in various ways. One useful and common approach is to determine a range of acceleration exposure that does not result in injury or death. The endpoint may be reached through various effects and at different levels for the whole body, or for specific body organs, structures, and systems.

There are three categories of impact. Whole-body impact is a generalized impact of the entire body as it occurs during an ejection or most laboratory tests. Penetrating impact is where an object penetrates a body part. Blunt impact is a focused nonpenetrating impact of a body part. Blunt impact and penetrating impacts may occur as a result of whole-body impact. Blunt, nonpenetrating impacts are common means of force application to restrained occupants of aircraft and spacecraft. Such forces are typically transmitted by seat surfaces, restraints, deforming cabin structures, and windblast. Localized blunt impact to inadequately restrained body parts may occur because of relative motion, which allows the body part to strike a fixed surface such as an instrument panel or a seat component. Therefore, whole-body acceleration effects, which involve generalized blunt impact, may secondarily include localized blunt impact.

Complex biological systems have multiple modes of injury. Most of the injury modes have little practical significance because the pathologic or lethal dose will be achieved by one mode before the others are reached at higher energy levels. In many cases a simple, single-degree-of-freedom model can be applied (60). In ejection seat design, such a single-degree-of-freedom model has been used to estimate the probability of injury in the lower spine. This injury normally occurs at a lower energy level than the energy required for other injuries.

Analysis of transient acceleration has been improved through research involving thousands of impact tests of human volunteers. The facilities now used for impact experiments include (i) towers that are used to drop test carriages onto decelerators such as metal-deforming devices or hydraulic cylinders, (ii) horizontal test tracks with various propulsion systems to propel test carriages into decelerators, and (iii) high-pressure gas actuators that accelerate a test carriage along either vertical or horizontal rails.

Comparison of test data collected from different impact facilities must be undertaken cautiously. Factors such as body support, restraint-system configuration, restraint pretension, subject bracing, prepositioning, waveform shape, and differences in data reference frames must be considered. The conditions imposed by the research device before the impact are critical (e.g., freefall tower vs. horizontal decelerator). When dynamic preloading, body positioning, muscle straining, and pretensioned restraints are employed, the results may not reflect actual in-aircraft results (61).

Summaries of portions of the historical tolerance database are available and can serve as useful guides to the literature (62,63). Extensive testing has also been

accomplished using cadavers and anthropomorphic test devices (crash test dummies) and these results are also compiled in the database. The findings of these studies provide much useful information and insight (64). A brief summary is presented in the subsequent text.

## Headward Acceleration (+G<sub>z</sub>)

The limiting factor for exposure of humans to +G<sub>z</sub> impact is vertebral fracture(s) in the lower thoracic and/or the lumbar region. Early investigators estimated that acceleration levels of +18 to +20 G<sub>z</sub>, with a velocity change of up to 17.5 m/s, could be tolerated without injury (65). USAF operational experience with ejection seats from 1949 to 1966 has shown that using these estimates as maximums for ejection catapult designs was reasonable, although not without injuries. For example, a review of 175 ejections from four aircraft producing peak acceleration levels of +17.5 to +18.4 G<sub>z</sub> over 0.1 to 0.18 seconds, with velocity changes of 15.2 to 25.9 m/s, revealed a 7% incidence of vertebral compression fractures. A more comprehensive analysis of the larger set of operational data, using a single-degree-of-freedom model of the lower spine, led to the development of a method to estimate the probability of spinal injury during ejection (60).

Hard landings and crashes in helicopters have a greater component of +G<sub>z</sub> acceleration than the primarily -G<sub>x</sub> acceleration of fixed wing aircraft, and (as in all aircraft crashes) blunt trauma is the primary cause of death. The use of a shoulder harness affords protection against some injuries. In addition, in a survivable vertical impact, the use of a stroking crew seat has been shown to prevent spinal injury (66).

## Footward Acceleration (-G<sub>z</sub>)

Spinal injury is also the limiting factor for -G<sub>z</sub> when the applied acceleration is compressive, as in a headfirst water impact, but the area at risk is the neck. In a downward ejection seat, the resulting force is partly in traction, through the pelvis by the lap belt, and partly in compression, by the restraint shoulder straps. Under these conditions, volunteers have routinely tolerated half-sine wave acceleration profiles up to -10 G<sub>z</sub> with times to peak acceleration ranging from 0.017 to 0.114 second and velocity changes of 1.5 to 15.4 m/s (67). Subjects in a rigid couch, restrained by two shoulder straps, a cross-chest strap, lap belt, crotch strap, and leg straps, tolerated peak accelerations up to -18.5 G<sub>z</sub> with a velocity change of 5.94 m/s (68).

## Transverse Rearward-Facing Impact (+G<sub>x</sub>)

A restraining surface, such as a seatback, allows tolerance to very high onset rates when the acceleration vector is oriented in the +x axis. In aviation, this is most applicable to rear-facing occupants during a frontal crash. Beeding and Mosely exposed a subject to a peak acceleration of +40.4 G<sub>x</sub> with a velocity change of 14.8 m/s and rate of onset of 2,139 G/s, with time to peak acceleration of 0.022 second, on a horizontal track decelerator. Special restraints and an

element of dynamic preload were involved. Symptoms of shock, including loss of consciousness after the test, were experienced (69), but the subject survived.

### Transverse Forward-Facing Impact ( $-G_x$ )

Perhaps the most dramatic human impact test experiences in any axis were those of Stapp and his colleagues, in a series of rocket sled studies published in 1951 (70). The highest acceleration exposure in this series was a  $-45.4 G_x$  run (45.4 G peak,  $-37 G_x$  average), with a velocity change of 54 m/s, which was experienced by Stapp himself in a forward-facing seat. The test had a G-onset rate of 493 G/s and included dynamic preload of the subject, specially designed wide belt restraints, and preimpact flexion of the neck. After this test, unilateral retinal hemorrhage occurred which resulted in a visual field defect lasting 10 weeks.

The most severe pathophysiologic effects in this group of experiments, however, were observed in a test involving another subject at the lower level of  $-38.6 G_x$ , but at the considerably higher G-onset rate of 1,340 G/s. The subject experienced symptoms of shock, several episodes of syncope, and albuminuria for 6 hours. The limits of human tolerance in the  $-x$  axis are lower when the restraint system is less adequate, and in the absence of imposed dynamic preload.

### Lateral Acceleration ( $G_y$ )

Subjects restrained only by a lap belt have been exposed to sideward impact up to  $9.95 G_y$ , with a velocity change of 4.6 m/s (71). When a lap belt and double shoulder strap configuration was used, acceleration peaks up to  $11.7 G_y$ , with a velocity change of 4.5 m/s, were tolerated (72). Earlier tests had been preformed using a vertical deceleration tower to explore the human response to y-axis impact. The subjects were restrained on their sides in an individually contoured couch. Tests were conducted on right and left lateral directions. Accelerations were varied from 4.3 to  $21.6 G_y$  with impact velocities of 6.68 m/s. The test subjects' complaints and physiologic responses to these conditions suggested that neither subjective nor objective tolerance had been reached (73).

### Multidirectional Acceleration

Efforts to determine human exposure limits for impact directions involving more than one cardinal axis have been limited to a narrow range of conditions, body support, and restraint systems. One multidirectional acceleration experiment was conducted using a vertical deceleration tower where the preimpact condition was near-weightless of freefall. A second experiment was performed on a horizontal deceleration track with a dynamic preload of approximately 0.3 G due to track friction.

In the first experiment, seven acceleration vectors were explored: up 45 degrees, up 45 degrees and right 45 degrees, up 45 degrees and left 45 degrees, right 45 degrees, left 45 degrees, left 90 degrees, right 90 degrees. Metal panels supported the subject's head, torso, and legs. Six acceleration profiles were used ranging from 3 to 26 G. Impact velocities

ranged from 1.5 to 8.6 m/s with rates of onset from 393 G/s to 1,380 G/s. Some temporary heart rhythm changes were noted immediately after four tests, but the tests were considered tolerable (73).

In the horizontal decelerator protocol, the subject experienced acceleration from 1 of 24 different directions. These compromised eight acceleration directions arrayed around the coronal plane, eight arrayed around a cone 45 degrees anterior to that plane, and eight arrayed in a cone 45 degrees posterior to the plane. Maximum repetitions ranged from 11.1 G for the  $-z$  axis to 30.7 G when the acceleration vector was acting from chest to back ( $-x$  axis) and 45 degrees left. Impact velocities were varied up to 13.7 m/s. None of these tests exceeded voluntary tolerance, but transitory postimpact bradycardia was a consistent finding for those impact vectors in which a component acted in the  $-z$  axis (74).

Useful data, which cannot be obtained from research on volunteer experimental subjects, have been gleaned from motor sport crashes since crash data recording was instituted in 2002 in the top three National Association for Stock Car Auto Racing (NASCAR) series race cars (75). Oblique frontal impacts have been experienced without serious injury when peak accelerations substantially exceeded those reported by Stapp, reaching 80 G but with a lower velocity change of approximately 34 m/s (76).

### Impact Attenuation

Impact attenuation is accomplished when the forces transmitted between the acceleration source and the occupant are limited to less than the levels that would be experienced if the occupant was rigidly coupled to that source. The acceleration being transmitted to a vehicle occupant may be attenuated by vehicle structural deformation, impact-attenuation devices between the seat and the vehicle, body support and restraint materials, and impact-attenuating materials within equipment such as a flight helmet.

In a moderately severe crash, acceleration is attenuated by the energy required to deform or crush structural components. The attenuation provided by structural crush is a major factor in crash protection, because relatively large attenuation distances are available. Vehicles at risk of crashing vertically, such as helicopters, use seat-mounted impact devices intended to attenuate the acceleration of the vehicle (Figure 4-16). Energy storage and rebound is usually avoided by using viscous or friction damping, or by permanently deforming materials such as metal tubes or bands.

If the impact velocity exceeds the capability of the attenuation device, the stroke limit will be reached and the phenomenon of bottoming occurs. The acceleration of the occupant will increase until the velocity of the vehicle is reached, as demonstrated in the plots in Figure 4-17.

Commonly used impact-attenuation devices may also have other properties that limit their usefulness. Some employ force-limiting mechanisms, so that their performance will vary as a function of occupant weight. The degree of impact attenuation that can be provided by the body support and restraint system, or by padding that might be worn by

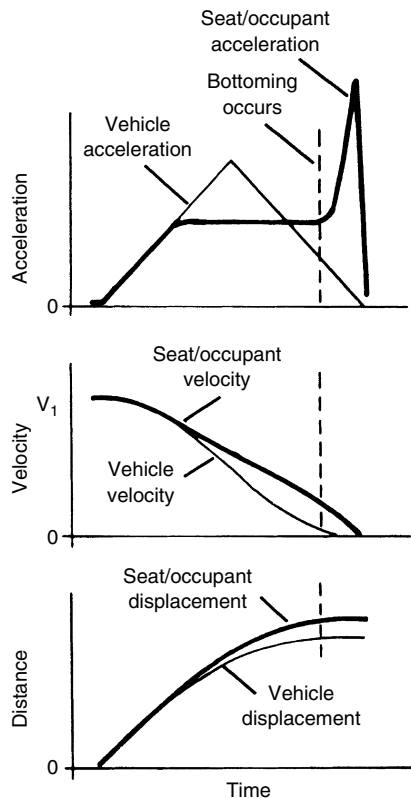


**FIGURE 4-17** Bottoming. When the attenuation device capability is exceeded, bottoming occurs with the potential of very high acceleration and high forces occurring. Injury potential is therefore enhanced. These plots show subject and vehicle displacements, velocities, and accelerations during an impact. Note the high-G peak on the upper plot when bottoming occurs.

an individual, is typically limited by the small displacements that are available.

## Restraints

The effectiveness of a restraint system depends on how well it transmits loads between the seat or vehicle structure and the occupant (while managing contact stresses). It also depends on the ability of the restraint to control the motion of restrained anatomic segments.

The first and most common restraint, the lap belt, provides a relatively low level of impact protection. The restraint loads are intended to be carried through the bones of the pelvis with the belt applied to the anterior superior iliac spines. If the belt is improperly tightened or positioned, or the acceleration vector is oriented to cause rotation of the pelvis, the belt can slip over the iliac crests to be against the abdomen. If this occurs, the belt loads will be applied against the lumbar spine with the abdominal organs interposed. When a lap belt is the only restraint, the most common injuries are the result of impact of the head and extremities within the vehicle.

The use of shoulder straps reduces the likelihood of an occupant striking the aircraft interior. In addition, they restrain forward movement of the torso during  $-G_x$  acceleration, and may reduce the strike envelope for sideward

and vertical impacts. The use of shoulder straps improves human tolerance to acceleration in any other direction by increasing the restraint-bearing area, increasing the number of anchor points for the torso mass, and reducing the relative motion between body parts. Where high upward acceleration components are anticipated, shoulder straps may help maintain the initial alignment of load-carrying spinal vertebrae.

Despite the advantages of shoulder straps, the tension loads create a potentially serious problem if they are attached to the center of the lap belt, as they are in many military harness configurations. These strap loads, developed under forward-facing impact conditions, lift the lap belt over the pelvis, allowing the belt to bear on the abdomen and the inferior costal margin. This problem has been observed in human tests at acceleration levels as low as 10 G with a velocity change of 5.5 m/s. Stapp reported that test subjects reached the threshold of voluntary tolerance with this restraint configuration at 17 G for impact velocities greater than 30 m/s (70). Some contemporary restraint harnesses include one or two straps that connect the lap belt buckle to the front central portion of the seat between the legs.

An example of a five-point restraint, currently in use in the space shuttle, is shown in Figure 4-18.

In view of the large influence that the restraint system has on tolerance to impact, the restraint configuration must be considered when interpreting human test results. For example, Stapp successfully demonstrated that humans are capable of tolerating acceleration levels up to  $-45.4 G_x$  in a forward-facing body position (70). The restraint system, however, was not a conventional military harness. A conventional military harness, composed of two 4.5-cm wide shoulder straps and a 7.6-cm wide lap belt, does not produce the effective coupling of various parts of the torso that the Stapp configuration provided. Unfortunately, a harness configuration of the type Stapp used has not been deemed practical in aerospace applications.

Efforts to develop a restraint system that will provide a high-bearing area and better control of body segment motion during impact have included the use of inflatable bags. This approach provides a restraint that does not encumber the vehicle occupant until the impact occurs. When predetermined acceleration levels are sensed on the vehicle structure, the airbag restraint is inflated by compressed gas, pyrotechnic gas generators, or a combination of the two systems. There has been concern that air bag deployments in aircraft could cause injuries due to interaction of the air bag with ancillary equipment such as night vision goggles (77). However, for crew positions not equipped with ejection seats, and for which head-mounted equipment is not used, inflatable bags may become practical.

Motor sport restraints typically include custom-fitted seats with multiple head and body side supports, side netting, helmets, head/neck restraints, and six- or seven-point restraint harness systems. Successful approaches have demonstrated reduction in neck tension load on the order of 80% as measured on test manikins (75). Some limitation in



**FIGURE 4-18** This five-point restraint harness is currently in use in the space shuttle. Similar designs are found in both military and civilian aircraft (NASA).

head and neck mobility is typically imposed, and the devices are usually employed in conjunction with some head side and rearward supports, which also impose visual obstructions. Conceptually, the devices provide an alternate load path in tension that decreases the tension load in the neck during frontal impacts. Although the potential for improvements based on the design of these systems exist, their application in most aerospace settings will be limited by mobility issues, visual restrictions, and the costly need for custom fit.

### Transient Acceleration Due to Escape Systems

The forces acting on the human body during emergency escape from high-speed aircraft include the thrust of the ejection seat catapult, the windstream surrounding the aircraft cockpit, the force exerted by the drogue parachute and the opening of the personnel recovery parachute. Ejection seats are complex mechanisms that need to balance a timely exit from the cockpit while avoiding excess accelerative forces.

Early ejection seats were propelled by cartridge-powered catapults to achieve seat trajectories that were adequate to clear the vertical tail of the aircraft and rescue airmen flying above 150 m. By the mid-1950s and early 1960s, rocket catapults were added to ejection seats. The objectives of the

rockets were (i) to reduce spinal injuries by permitting the ejection cartridge thrust to be reduced and (ii) sustaining the thrust after cockpit separation to achieve trajectories that might provide escape from zero altitude and zero speed. (78) The 1950s and 1960s also saw the development of automatic ejection sequencing including barometric control of parachute opening, automatic restraint release, seat separators, and control of the parachute opening by staged reefing.

An out-of-position ejection (for example, leaning forward) may lead to vertebral injuries due to the catapult thrust. With a lower body weight, the overall weight of the seat and crewmember may be less than the original design specifications. In that case, at a given thrust, the G-level attained by a smaller crewmember may be greater than is required to clear the aircraft, and may be beyond safe limits.

For all crewmembers who experience an ejection, once the canopy is cleared, impact from windblast may cause severe or even fatal injury at high air speeds. The force associated with windblast is proportional to the square of air speed, so ejection at 600 knots presents a force that is nine times greater than an ejection at 200 knots. When the ejection airspeed is in the range of 500 to 600 knots, aerodynamic acceleration may be as high as 30 to 40 G for a typical human body and ejection seat.

Windblast may also cause injury to an unrestrained arm or leg. The limb is dislodged from its initial position by a combination of drag and lift (and especially sideward lift). Rearward motion of the limb, so-called flailing, results from the inequality between the ratio of its mass and aerodynamic drag and the ratio of the occupant/seat combination and aerodynamic drag.

The types of injuries observed as a result of high-speed ejection include scleral hemorrhage, fractures, joint derangements of limbs, and distraction of the cervical spine. Other injuries can occur due to direct impact with the seat or other hard structures. Recent estimates place 80% of ejections within the safe envelope. Sixty-two percent of ejectees had minor injuries whereas 16% had major injuries (79).

### Seats and Seat Cushions

Aerospace designers have proposed that the ideal body support system is a rigid, individually contoured couch. This approach ensures that each external body segment will be simultaneously accelerated in the design direction, and that the support pressure exerted on the body surfaces will be minimized. Designs of this type have been found to be effective in laboratory impact, vibration, and centrifuge tests. The rigid contour approach was used in the Project Mercury astronaut couch design, and in the design of the seat and seatback used in Project Gemini. The disadvantages of the approach are the high cost of individual fitting and the discomfort of the rigid contour after a relatively short occupancy.

Attempts to circumvent the disadvantages of the rigid couch design have included the design of net couches. These

designs provide improved comfort and avoid the high manufacturing costs of rigid contour couches. Thus far, net body support systems have been found to be effective in sustained acceleration, but have not provided good protection in either vibration or impact. The problem has been related to the elasticity of the net material. In both vibration and impact tests, the net body suspension system tended to resonate at or near the natural frequencies of the body.

The most successful body support systems that have aerospace vehicle applications have (i) slight contouring to control body position, (ii) dimensions that accommodate large variations in body size, (iii) relatively rigid, lightweight structures, (iv) padding to provide isolation from small-amplitude, high-frequency impacts and vibration, and (v) minimal cushioning of the seat to reduce flight fatigue without major degradation in impact protection. Armrests are often provided to increase comfort.

One might predict that materials and structures such as soft cushions should always protect an individual during an impact, but that is not the case. Rather than lessen forces, materials positioned between the occupant and the acceleration source can amplify the acceleration to which the occupant will be exposed. First, the materials may store energy during the impact and then release it in rebound. Therefore, the occupant is exposed to a larger velocity change than the vehicle. Second, these deformations may delay the acceleration of the occupant and create a large velocity difference between the occupant and the vehicle. The occupant acceleration must subsequently exceed the vehicle acceleration to eliminate the velocity difference. An ejection seat cushion is a common component that can cause this second problem by virtue of its stiffness and the distance it creates between the seat structure and the seat occupant.

It is important for such viscoelastic pads to impart minimal additional acceleration to the crewmember during ejection. A spongy, soft pad can result in severe impact damage to the vertebral column if the seat accelerates several inches before the compressing pad allows the occupant to be impacted from below by the seat. The initial movement of the seat must be simultaneous with movement of the occupant if the full protective effect of a rocket powered ejection is to be realized. The seat pads on ejection seats feel rather stiff and sometimes uncomfortable to aircrew. Life-support officers and flight surgeons should fully understand the potential ejection risks when a crewmember uses additional unauthorized padding.

One solution to the problem of ejection seat cushion comfort involves “rate-limited foams.” Cushions made from this material slowly adapt to the pressure contour of the buttocks and provide comfort by eliminating “hot spots,” but they do not compress quickly enough to bottom out during ejection acceleration (80).

## Parachuting

In sport or operational use of parachutes, the opening force is transmitted to a parachutist through the risers and into the

harness. It is of relatively long duration, on the order of 1 to 2 seconds at an altitude of 300 m. Parachute forces involve two phases, the first related to line stretch and the second to actual opening shock. The magnitudes of the forces are a function of variables that include deployment velocity, air density, deployment orientation of the canopy, suspension line length, and mass of the parachutist.

Opening shock may be high at high altitudes and/or high speeds. For example, a 91kg parachutist at equilibrium velocity using an 8.5-m diameter, flat-panel, nylon parachute, will experience a force of 6,200 Newtons (N) at an altitude of 2,100 m. Greater forces will occur at higher altitudes (e.g., 14,700 N at an altitude of 12,200 m) (81). Because the incorporation of automatic parachute opening devices that delay parachute opening until an altitude of approximately 4,600 m, and the use of parachute canopy reefing, injuries due to parachute opening have become uncommon.

After completion of the parachute opening sequence and descent to the Earth’s surface, the parachutist confronts a final acceleration on ground impact. A typical military parachute will lower the parachutist to the Earth at a velocity of approximately 6.4 m/s. The landing impact is equivalent to that experienced after a jump from a height of 2.1 m. The resulting impact forces are a function of the effectiveness of the parachutist’s fall technique (that is, the ability to use the legs as impact attenuators), and of the direction and velocity of horizontal wind drift.

Injuries due to parachute opening and landing falls from freefall bailouts are uncommon in typical sport parachuting use for several reasons. First, the velocity and altitude of parachute opening are more controlled. Second, skydiving techniques are used to control the parachutist’s attitude at the time of opening. And third, steerable, gliding parafoil parachutes control landing altitude and final descent velocity.

## Crashes

When an aircraft strikes an object or terrain, a force acts on its structure that compels it to decelerate. The magnitude of this force may be sufficient to slow the aircraft from its initial impact speed, to a final speed, which may be zero. The magnitude of this opposing force depends on the length of time it has to act. If the time is short, a higher force will result. If the time is comparatively long, the force will be less.

The potential for injury and death in a crash relate to the forces. As depicted in Figure 4-15A and B, when aircraft deceleration is spread over a longer distance, average G can be less and injury potential may be reduced. Equation 12 related the G of an occupant fixed at the center of the aircraft with the velocity at impact and the deceleration distance.

To assess injury potential in crashes, many investigators start by determining the variables of velocity and crash distance. Crash velocity can sometimes be determined from flight data recorders, inspection of flight instruments (e.g., marks on the airspeed indicator), or the flight characteristics of the aircraft at impact (e.g., a stall or spin). The crash distance can be determined from scene evidence that includes

ground scars, aircraft crush, and seat stroking distance. A ground survey of the crash site and careful inspection of the wreckage can usually lead to reasonable estimates of this distance.

Equation 12 can then be used to develop an estimate of the *average* deceleration experienced by a person fixed within the aircraft. As discussed, the peak-G will be always be higher. Doubling the Equation 12 estimate is one approach to estimating peak-G. This assumes that the forces increased and decreased symmetrically during the crash and peaked in the middle. Other versions of Equation 12 have been developed that use different assumptions with regard to the timing of forces during the crash.

Because the estimated G is a vector, it must be reconciled with the position of the occupants within the aircraft, the flight path of aircraft, aircraft attitude, and other factors such as the slope of the impacted terrain. For example, a helicopter that autorotates and crashes will experience mainly vertically aligned forces. To a seated pilot, this would result in primarily  $+G_z$ . A person lying supine (like a medevac patient) would experience  $+G_x$  in the same event. Reconciliation of the G-vector to each occupant of the aircraft is possible using trigonometry.

It is important to remember that Equation 12 is specific for an occupant fixed to the aircraft. This ideal never occurs in reality and, as discussed in the section on kinematics, occupant motion will always occur during a crash. This motion is influenced by the restraints, seats, and surrounding structures. Injury relates to the G and points of contact of the occupant with the aircraft. By estimating and understanding the G-vector of the crash, an understanding of this motion is possible.

With this understanding, assessment of injuries and the role of restraints and other safety devices in causing or preventing injuries can be made. If the initial estimate of G, including direction, falls well within a survivable range, and serious injury or death nevertheless occurred, the circumstances of the crash and design of safety equipment will merit special scrutiny.

Identification of injury mechanisms should meet the following criteria: (i) the load transmission path from seat structure and restraints to the point of injury should be understood; (ii) the load transmission path should be in accordance with physical principles by taking into account the origins of the loads, the motions of the transmitting structure under loading, and the capability of the transmitting structure to carry the loads; and (iii) the transmitted load should produce sufficient stress at the appropriate point to account for the injury.

### Future Directions

Opportunities exist to enhance impact protection within the aerospace environment. One future challenge lies in the area of neck protection of crew wearing head-mounted equipment such as advanced optical displays, vision aids, and laser eye protection. These systems add weight and change the center of gravity of the head/helmet, which can significantly

increase cervical stress during maneuvering acceleration, crash, or escape. A variety of alternate load path protective modalities for the head or helmet have been proposed. Some form of inflatable neck collar may offer potential benefit. Interventions being considered should be judged against the risks of what is emerging as a better understanding of injury criteria.

Other challenges include the need to clearly define gender differences in impact tolerance and impact protection requirements. Young adult females have an approximately 22% increased risk of death from matched vehicular crash forces (82). This challenge may be particularly relevant to space exploration and the expected forces that will be encountered during capsule recovery involving astronauts of both genders. Escape modules, including space capsules, can involve significant morbidity at ground impact after parachute descent (83).

Further efforts to provide personnel protection for military aviation should see the application of automated aircraft ground avoidance flight control systems, automatic ejection decision-making electronics, and the development and use of microprocessors designed to tailor the escape system performance to prevailing conditions. New technologies that will support such tailoring may include ejection catapults incorporating a dynamic preload phase (61), adjustment of ejection catapult thrust to accommodate different sizes of seat occupants, and parachutes with variable drag and lift characteristics.

Equipment worn by the occupant will become more complex and will integrate multiple functions including the anti-G suit, restraint, windblast protection, antiexposure provisions, environmental sensing, flotation, and protection from biological and chemical agents. The personnel protection ensemble and the means of emergency escape should be developed and tested as an integrated system to exploit potential synergies and avoid duplication and mismatches.

Several nations are currently engaged in the development of space vehicles that will carry crews into Earth's orbit, to the lunar surface, and in the case of the United States, interplanetary exploration. An issue that must be addressed more completely in these new space flight ventures is the influence of diminished bone and muscle strength on tolerance to abrupt acceleration after long-duration flights. The decision to retire the STS space shuttles and return to the capsule concept containing up to six crewmembers will provide significant design challenges over the next few years. The unprecedented number of crew in one capsule exposed to parachute recovery acceleration and landing impact will require concentrated and rigorous investigation and design.

With the advent of commercial space tourism, high-altitude military flight operations, and the near-term continued use of the STS space shuttle, the problem of high-altitude escape remains a challenge. Military aircraft capable of high altitude have employed ejection seats (with full pressure suits) and self-contained escape capsules. To



escape the space shuttle, astronauts must unstrap from their seats, make their way to the main deck escape hatch, deploy a bailout pole, attach their parachute lanyard to the pole, and exit the craft. The system offers an escape option below 12,200 m altitude.

In the design of flight suits and anti-G garments for aircraft, it is important that inflated bladders are not used between the crewmember and an ejection seat. Helmets and clothing should be designed so as to not cause excessive lift and consequent injury at high air speed. For astronauts returning from ballistic or orbital flight, garments must serve the purpose of protection against loss of pressure and still be compatible with escape systems.

Lessons learned from earlier spacecraft designs may be applicable to these endeavors. Nevertheless, many design and personnel protection challenges remain, and several exist as a result of the multiuse of protective equipment that has been developed primarily for a different set of aerospace system design requirements. Pressure suits provide an example. A suit designed to provide protection within the context of a lifting body spacecraft design, where launch and entry accelerations are relatively low, may not be an appropriate design for a ballistic entry vehicle. Many aspects of a high-mobility suit, designed for space pressures, may not be appropriate during the higher accelerations associated with emergency egress during a flight, or during landing impact. These aspects may include the design of the helmet, the neck ring, or the difficulty of providing adequate torso restraint that is compatible with a full pressure suit. It will remain difficult to achieve a predictably successful protective system design, within a given design context, because so many factors must be considered. The relative importance of each factor may be perceived differently by vehicle designers and escape system designers.

Modeling and simulation will continue to evolve with improvements in computer microprocessors and memory. The automotive industry has taken the lead in the creation of human injury models and it may be possible to exploit these applications. These models are usually validated against cadavers or Anthropometric Test Devices. However, adjustment of injury parameters must be made for the different populations at risk as well as the differences in restraint, body support, and head protection. Because neither of these truly represents living people, use and application must be viewed with continued caution.

## ACKNOWLEDGMENTS

The authors wish to acknowledge the important contributions of Sidney D. Leverett, James E. Whinnery, Russell R. Burton, and James H. Raddin, Jr. As authors of chapters on sustained and transient acceleration found in previous editions of this textbook, they provided much of the foundational content of this work. Mr. John Martini, an illustrator at Biodynamic Research Corporation, created and edited many of the figures and tables.

## REFERENCES

1. Fryer DI. *Glossary of aerospace terms*. AGARDograph No 153. Aerospace Medicine Panel, 1971.
2. Gell CF. Table of equivalents for acceleration terminology. *Aerosp Med* 1961;32: 1109–1111.
3. Kaufman WC, Baumgardner FW, Gillingham KK, et al. Standardization of units and symbols: revised. *Aviat Space Environ Med* 1984;55: 93–100.
4. Wood EH, Sturm RE. Human centrifuge non-invasive measurements of arterial pressure at eye level during  $G_z$  acceleration. *Aviat Space Environ Med* 1989;60: 1005–1010.
5. Rossen R, Kabat H, Anderson JP. Acute arrest of the cerebral circulation in man. *Arch Neurol Psychiatry* 1943;50: 510–528.
6. Beckman EL, Duane TD, Ziegler JE, et al. Some observations on human tolerance to accelerative stress: phase IV. Human tolerance to high positive G applied at a rate of 5 to 10 G per second. *J Aviat Med* 1954;25: 50–66.
7. Wood EH. Some effects of the force environment on the heart, lungs and circulation. *Clin Invest Med* 1987;10: 401–427.
8. Banks RD, Gray G. “Bunt bradycardia”: two cases of slowing of heart rate in flight during  $-G_z$ . *Aviat Space Environ Med* 1994;65: 330–331.
9. Banks RD, Grissett JD, Turnipseed GT, et al. The “push-pull effect”. *Aviat Space Environ Med* 1994;65: 699–704.
10. Ryan EA, Kerr WK, Franks WR. Some physiological findings on normal men subjected to negative G. *J Aviat Med* 1950;21: 173–194.
11. Burton RR, Storm WF, Johnson LW, et al. Stress responses of pilots flying high-performance aircraft during aerial combat maneuvers. *Aviat Space Environ Med* 1977;48: 301–307.
12. Glaister DH. *The effects of gravity and acceleration on the lung*. AGARDograph 133. England: Technivision Services, 1970.
13. Burns JW, Ivan DJ, Stern CH, et al. Protection to +12  $G_z$ . *Aviat Space Environ Med* 2001;72: 413–421.
14. Shender BS, Forester EM, Hrebien L, et al. Acceleration-induced near-loss of consciousness: the “A-LOC” syndrome. *Aviat Space Environ Med* 2003;74: 1021–1028.
15. Burton RR. G-induced loss of consciousness: definition, history, current status. *Aviat Space Environ Med* 1988;59: 2–5.
16. Cochran LB, Gard PW, Norsworthy ME. *Variations in human G tolerance to positive acceleration* USN SAM/NASA/NM 001–059.020.10. Pensacola, 1954.
17. Code CF, Wood EH, Lambert EH, et al. Interim progress reports and concluding summary of 1942–46 acceleration physiology studies. In: Wood EH, ed. *Evolution of anti-G suits and their limitations, and alternative methods for avoidance of G-induced loss of consciousness*. Rochester: Mayo Foundation Special Purpose Processor Development Group, 1990: 409–430.
18. Navathe PD, Gomez G, Krishnamurthy A. Relaxed acceleration tolerance in female pilot trainees. *Aviat Space Environ Med* 2002;73: 1106–1108.
19. Heaps CL, Fischer MD, Hill RC. Female acceleration tolerance: effects of menstrual state and physical condition. *Aviat Space Environ Med* 1997;78: 525–530.
20. Hearon CM, Fischer MD, Dooley JW. Male/female SACM endurance comparison: support for the Armstrong Laboratory modifications to the CSU-13B/P anti-G suit. *Aviat Space Environ Med* 1998;69: 1141–1145.
21. Eiken O, Tipton MJ, Kölegård R, et al. Motion sickness decreases arterial pressure and therefore acceleration tolerance. *Aviat Space Environ Med* 2005;76: 541–546.
22. Tripp LD. *Use of lower body negative pressure as a countermeasure to negative  $G_z$  acceleration*. Wright-Patterson Air Force Base: United States Air Force, 1989.
23. Rushmer RF, Beckman EL, Lee D. Protection of the cerebral circulation by the cerebrospinal fluid under the influence of radial acceleration. *Am J Physiol* 1947;151: 355–365.

24. Banks RD, Grissett JD, Saunders PL, et al. The effect of varying time at  $-G_z$  on subsequent  $+G_z$  physiological tolerance (push-pull effect). *Aviat Space Environ Med* 1995;66: 723–727.
25. Goodman LS, Banks RD, Grissett JD, et al. Heart rate and blood pressure responses to  $+G_z$  following varied-duration  $-G_z$ . *Aviat Space Environ Med* 2000;71: 137–141.
26. Goodman LS, LeSage S. Impairment of cardiovascular and vasomotor responses during tilt table simulation of “push-pull” maneuvers. *Aviat Space Environ Med* 2002;73: 971–979.
27. Kobayashi A, Tong A, Kikukawa A. Technical Note: pilot cerebral oxygen status during air-to-air combat maneuvering. *Aviat Space Environ Med* 2002;73: 919–924.
28. Rogers TA, Smedal HA. The ventilatory advantage of backward transverse acceleration. *Aerosp Med* 1961;32: 737–740.
29. Nolan AC, Marshall HW, Cronin L, et al. Decreases in arterial oxygen saturation and associated changes in pressures and roentgenographic appearance of the thorax during forward ( $+G_x$ ) acceleration. *Aerosp Med* 1963;34: 797–813.
30. Clarke NP, Bondurant S, Leverett SD. Human tolerance to prolonged forward and backward acceleration. *J Aviat Med* 1959;30: 1–21.
31. Harding RM. *Survival in space: medical problems of manned spaceflight*. London and New York: Routledge, 1989.
32. Hershgold EJ. Roentgenographic study of human subjects during transverse acceleration. *Aerosp Med* 1960;31: 213–219.
33. Popplow JR, Veghte JH, Hudson KE. Cardiopulmonary responses to combined lateral and vertical acceleration. *Aviat Space Environ Med* 1983;54: 632–636.
34. Albery WB. Acceleration in other axes affects  $+G_z$  tolerance: dynamic centrifuge simulation of agile flight. *Aviat Space Environ Med* 2004;75: 1–6.
35. Green ND, Ford SA. G-induced loss of consciousness: retrospective survey results from 2259 military aircrew. *Aviat Space Environ Med* 2006;77: 619–623.
36. Burton RR, Whinnery JE. Biodynamics: sustained acceleration. In: DeHart RL, Davis JR, eds. *Fundamentals of aerospace medicine*. Philadelphia: Lippincott Williams & Wilkins, 2002.
37. Lyons TJ, Craft NO, Copley GB, et al. Analysis of mission and aircraft factors in G-induced loss of consciousness in the USAF: 1982–2002. *Aviat Space Environ Med* 2004;75: 479–482.
38. Sevilla NL, Gardner JW. G-induced loss of consciousness: case-control study of 78 G-LOCs in the F-15, F-16, and A-10. *Aviat Space Environ Med* 2005;76: 370–374.
39. Michaud VJ, Lyons TJ. The “push-pull effect” and G-induced loss of consciousness accidents in the U.S. Air Force. *Aviat Space Environ Med* 1998;69: 1104–1106.
40. Mohler SR. *G effects of the pilot during aerobatics*. Washington, DC: Federal Aviation Administration, Office of Aviation Medicine, 1972.
41. Shender BS. Human tolerance to  $G_z$  acceleration loads generated in high-performance helicopters. *Aviat Space Environ Med* 2001;72: 693–703.
42. Drane M, Navathe PD, Preitner CG, et al. G-LOC in general aviation (abstract). *Aviat Space Environ Med* 2007;78: 225.
43. Wood EH, Satterer WF, Marshal HW, et al. *Effect of headward and forward accelerations on the cardiovascular system*. Wright-Patterson AFB, Dayton, Ohio: Aerospace Medical Laboratory, 1961.
44. Wood EH. Contributions of aeromedical research to flight and biomedical science. *Aviat Space Environ Med* 1986;57(Suppl 10): A13–A23.
45. Mikuliszyn R, Zebrowski M, Kowalczyk K. Centrifuge training program with “push-pull” elements. *Aviat Space Environ Med* 2005;76: 493–495.
46. Balldin UI, Werchan PM, French J, et al. Endurance and performance during multiple intense high  $+G_z$  exposures with effective anti-G protection. *Aviat Space Environ Med* 2003;74: 303–308.
47. Laughlin HM. An analysis of the risk of human cardiac damage during  $+G_z$  stress: a review. *Aviat Space Environ Med* 1982;53: 423–431.
48. AGARD Aerospace Medical Panel Working Group 18. Echocardiographic findings in NATO pilots: do acceleration ( $+G_z$ ) stresses damage the heart? *Aviat Space Environ Med* 1997;68: 596–600.
49. Haswell MS, Tacker WA, Balldin UI, et al. Influence of inspired oxygen concentration on acceleration atelectasis. *Aviat Space Environ Med* 1986;57: 432–437.
50. Beyer RW, Dailey PO. Renal artery dissection associated with  $G_z$  acceleration. *Aviat Space Environ Med* 2004;75: 284–287.
51. Snyder QC, Kearney PJ. High  $+G_z$  induced acute inguinal herniation in an F-16 aircrew member: case report and review. *Aviat Space Environ Med* 2002;73: 68–72.
52. Landau D-A, Chapnick L, Yoffe N, et al. Cervical and Lumbar MRI findings in aviators as a function of aircraft type. *Aviat Space Environ Med* 2006;77: 1158–1161.
53. Newman DG, Callister R. Analysis of the  $G_z$  environment during air combat maneuvering in the F/A-18 fighter aircraft. *Aviat Space Environ Med* 1999;70: 310–315.
54. Michaud V, Lyons T, Hansen C. Frequency of the “push-pull effect” in U.S. Air Force fighter operations. *Aviat Space Environ Med* 1998;69: 1083–1086.
55. Lyons TJ, Banks RD, Firth J. Introduction. *Human consequences of agile aircraft, RTO Lecture Series 220*, RTO-EN-12. Neuilly-sur-seine Cedex, France: Research and Technology Organization, 2000: I–I–9.
56. Buckley JC. Cardiovascular changes: atrophy, arrhythmias, and orthostatic intolerance. *Space physiology*. New York: Oxford University Press, 2006: 139–167.
57. Perez SA, Charles JB, Fortner GW, et al. Cardiovascular effects of anti-G suit and cooling garment during space shuttle re-entry and landing. *Aviat Space Environ Med* 2003;74: 753–757.
58. Stoll AM. Human tolerance of positive G as determined by the physiological end points. *J Aviat Med* 1956;27: 356–367.
59. Rogers, D. Model derived timing requirements for  $G_z$  protection methods. *Models for aircrew safety assessment: uses, limitations and requirements*. RTO Meeting Proceedings 20, RTO-MP-20. Neuilly-sur-seine Cedex, France: Research and Technology Organization, 1999: 22–1–22–6.
60. Brinkley JW, Shaffer JT. Dynamic simulation techniques for the design of escape systems: Current applications and future Air Force requirements. *Biodynamic models and their applications*. Wright-Patterson Air Force Base, Ohio: Aerospace Medical Research Laboratory, 1971.
61. Hearon BF, Raddin JH, Brinkley JW. Evidence for the utilization of dynamic preload in impact injury prevention. *Impact injury caused by linear acceleration: mechanisms, prevention and cost*. AGARD Conference Proceedings No 322. AGARD-CP-322, 1982: 31–1–31–14.
62. von Gierke HE, Brinkley JW. Impact accelerations. In: Calvin J, Gazenko O, eds. *Foundations of space biology and medicine*, joint USA/USSR publication. Washington, DC: National Aeronautics and Space Administration, 1975: 214–246.
63. Snyder RG. Impact. In: Parker JF, Weeds VR, eds. *Bioastronautics data book*. NASA SP-3006. Washington, DC: National Aeronautics and Space Administration, 1973: 221–295.
64. Cheng H, Buhman JR. *Development of the biodynamics data bank and the web user interface*. SAE 2000-01-0162. Warrendale: SAE International, 2000.
65. Lovelace W, Baldes E, Wulff V. *The ejection seat for emergency escape from high-speed aircraft*. ASTIA ATI, 7245, 1945.
66. Shanahan DF. *Basic principles of helicopter crashworthiness*. USAARL 93–15. Fort Rucker: United States Army Aeromedical Research Laboratory, 1993.
67. Brinkley JW, Getschow K. Escape system design criteria based on human response to  $-z$  axis acceleration. SAFE Association. 1988.

- Data and paper available at: [www.biodyn.wpafb.af.mil/GenStyInfo.asp?sn=198504](http://www.biodyn.wpafb.af.mil/GenStyInfo.asp?sn=198504).
68. Shulman M, Critz GW, Highly FM, et al. *Determination of human tolerance to negative impact acceleration*. UAEC-ACEL-510. Philadelphia: US Naval Air Engineering Center, 1963.
  69. Beeding EL, Mosley JD. *Human tolerance to ultra-high G forces*. AFMDC-TN-60-2. Holloman Air Force Base: Aeromedical Field Laboratory, Air Force Missile Development Center, 1960.
  70. Stapp JP. *Human exposures to linear deceleration. Part 2: the forward-facing position and the development of a crash harness*. Air Force Technical Report 5915. Wright-Patterson Air Force Base, Ohio: Aero Medical Laboratory, Wright Air Development Center, 1951.
  71. Zaborowski AV. Human tolerance to lateral impact with lap belt only. *The eighth Stapp car crash and field demonstration conference*. Detroit: Wayne State University Press, 1966: 34–71.
  72. Zaborowski AV. Lateral impact studies: lap belt-shoulder harness investigation. *The ninth Stapp car crash proceedings*. Minneapolis: University of Minnesota, 1966: 93–127.
  73. Weis EB, Clark NP, Brinkley JW. Human response to several impact acceleration orientations and patterns. *Aerosp Med* 1963;34: 1122–1129.
  74. Brown WK, Rothstein JD, Foster P. Human response to predicted Apollo landing impacts in selected body orientations. *Aerosp Med* 1966;37: 394–398.
  75. Gramling H, Hodgman P, Hubbard R. Development of the HANS head and neck support for Formula One. *1998 Motor sports engineering conference proceedings*. SAE 983060. Warrendale, PA: Society of Automotive Engineers, 1998.
  76. Melvin JW, Begemen PC, Faller RK, et al. Crash protection of stock car racing drivers—application of biomechanical analysis of Indy car crash research. *Stapp Car Crash J* 2006;50: 415–428.
  77. Power ED, Duma SM, Stitzel JD, et al. Computer modeling of airbag-induced ocular injury in pilots wearing night vision goggles. *Aviat Space Environ Med* 2002;73: 1000–1006.
  78. Anton D. Aviation: injuries and protection. In: Cooper G, ed. *Scientific foundations of trauma*. Oxford: Butterworth-Heinemann, 1997: 172–188.
  79. Hunt JC, Johanson DC. Ejection mortality and morbidity: what are the odds of being killed or injured during ejection? A first look, with trends. (abstract). *Aviat Space Environ Med* 2006;77: 322.
  80. Hearon BF, Brinkley JW. Effect of seat cushions on human response to +G<sub>z</sub> impact. *Aviat Space Environ Med* 1986;57: 113–121.
  81. Hallenbeck GA. *The magnitude and duration of parachute opening shock at various altitudes and air speeds*. ENG-49-696-66. Dayton, Ohio: Army Air Forces Materiel Command, Engineering Division, Aero Medical Laboratory, 1944.
  82. Evans L, Gerrish PH. *Gender and age influence on fatality risk from the same physical impact determined using two-car crashes*. SAE 2001-01-1174. Warrendale: SAE International, 2001.
  83. Hearon BF, Brinkley JW, Luciani RJ, et al. *F/FB-111 Ejection experience (1967–1980)—Part I: evaluation and recommendations*. AFAMRL-TR-81-113. Wright-Patterson AFB, Ohio: Air Force Aerospace Medical Research Laboratory, 1981.

## RECOMMENDED READINGS

---

- Buckey JC. Cardiovascular changes: atrophy, arrhythmias, and orthostatic intolerance. *Space physiology*. New York: Oxford University Press, 2006: 139–167.
- Fryer DI. *Glossary of aerospace terms*. AGARDograph No 153. Aerospace Medicine Panel, 1971.
- Glaister DH. *The effects of gravity and acceleration on the lung*. AGARDograph 133. England: Technivision Services, 1970.
- Shanahan DF. *Basic principles of helicopter crashworthiness*. USAARL 93–15. Fort Rucker: United States Army Aeromedical Research Laboratory, 1993.
- Stapp JP. *Human exposures to linear deceleration. Part 2: the forward-facing position and the development of a crash harness*. Air Force Technical Report 5915. Wright-Patterson Air Force Base, Ohio: Aero Medical Laboratory, Wright Air Development Center, 1951.
- Wood EH. *Evolution of anti-G suits and their limitations, and alternative methods for avoidance of G-induced loss of consciousness*. Rochester: Mayo Foundation Special Purpose Processor Development Group, 1990.